Communication in Physical Sciences, 2026, 13(6):915-947

Grain Size Distribution Patterns within the Calabar River: Implications for Paleoenvironmental Reconstruction

Chimezie Emeka, Victoria Emeka, Edak Agi-Odey, Aniekan Ukpe, and Celsus Agim
Received: 26 March 2026/Accepted: 25 May 2026 /Published: 04 June 2026
https://dx.doi.org/10.4314/cps.v13i6.6

Abstract: *This study investigated sediment distribution patterns within the Calabar River, southeastern Nigeria, with the aim of improving the recognition of tidal facies and enhancing paleoenvironmental reconstruction of ancient estuarine deposits. A total of 50 geo-referenced bottom sediment samples were collected in September 2011 using a Van Veen grab sampler along a 24 km tidal channel covering approximately 17.45 km². Tidal current measurements and bathymetric surveys were conducted during spring, mean, and neap tidal cycles. Maximum surface current velocities ranged from 0.41 to 0.61 m s⁻¹ at Adiabo Bridge and from 0.65 to 0.95 m s⁻¹ at Marina Beach, while near-bottom velocities varied from 0.27 to 0.43 m s⁻¹ and 0.46 to 0.67 m s⁻¹, respectively. Velocity profiles revealed an ebb-dominant hydrodynamic regime indicative of tidal asymmetry and net seaward sediment transport. Bathymetric analysis showed channel depths ranging from 2 to 20 m, with the deepest sections occurring within the central channel. Grain-size analysis revealed predominantly bimodal distributions comprising mud, sand, gravel, and mixed sediment fractions. Textural classification showed that sand and muddy sand constitute the dominant sediment types throughout the river system. Statistical analyses of mean grain size, sorting, skewness, and kurtosis indicated strong spatial variability linked to hydrodynamic energy conditions and sediment transport processes. Three sedimentary facies were identified: Facies A (upstream), extending approximately 6 km and characterized by fine-grained sands and muddy sands deposited under flood-dominated conditions; Facies B (central), extending approximately 8 km and dominated by medium sands with gravelly patches associated with maximum tidal energy and depths reaching 20 m; and Facies C (downstream), extending approximately 10 km and consisting mainly of medium sands and muddy sands deposited under ebb-dominated conditions. The facies succession reflects the combined influence of tidal asymmetry, channel morphology, and sediment supply on sediment distribution. These findings demonstrate that grain-size statistical parameters provide reliable indicators of depositional processes and facies architecture in meso-tidal rivers. The Calabar River therefore serves as an important modern analogue for interpreting ancient tidal-channel and estuarine deposits preserved in the geological record.*

Keywords: *Tidal asymmetry, grain size analysis, sediment facies, bathymetry, river sediment dynamics*

Chimezie Emeka
Department of Geology, University of Calabar, P.M.B. 1115, Calabar, Nigeria
Email: emekachimezie@unical.edu.ng
https://orcid.org/0000-0002-5383-686X
Victoria Emeka
Faculty of Oceanography, University of Calabar, P.M.B. 1115, Calabar, Nigeria
Email: emekavictoria@unical.edu.ng
https://orcid.org/0000-0002-5603-7131
Edak Agi-Odey
Faculty of Oceanography, University of Calabar, P.M.B. 1115, Calabar, Nigeria
Email: edakefiom@gmail.com
https://orcid.org/0000-0003-4708-0143
Aniekan Ukpe
Department of Geology, University of Calabar, P.M.B. 1115, Calabar, Nigeria
Email: ukpe22.ng@gmail.com

Celsus Agim
Faculty of Oceanography, University of Calabar, P.M.B. 1115, Calabar, Nigeria
Email: celsusagim111@gmail.com

1.0 Introduction

Tidal rivers represent dynamic coastal sedimentary environments shaped by the Holocene rise in sea level. Their evolution is controlled by the interplay of tides, waves, and fluvial processes. A tidal river may be defined as a tidally influenced fresh to slightly brackish water channel that does not directly open into the sea but exhibits both fluvial and tidal facies (Dalrymple & Choi, 2007).

The sedimentary records preserved within tidal rivers provide valuable archives of environmental change and are increasingly used as modern analogues for interpreting ancient estuarine and coastal deposits. Understanding the spatial distribution of sediment textures and facies in modern tidal systems is therefore essential for reconstructing past depositional environments, relative sea-level changes, and basin evolution.Sediment distribution within tidal rivers is largely a function of tidal strength and fluvial discharge, making them highly efficient sediment traps (Biggs & Howell, 1984). Rates of transport and accumulation are strongly influenced by tidal currents and river inflows (Hall et al., 1987 Nichols & Biggs, 1985).

The interaction between fluvial discharge and tidal forcing produces complex patterns of sediment erosion, transport, and deposition. These processes generate distinctive textural signatures that can be preserved within the sedimentary record and subsequently used to infer hydrodynamic conditions that prevailed during deposition.

Grain size statistical parameters have long been employed to characterize depositional environments (Folk & Ward, 1957; Friedman, 1961; Malvarez et al., 2001; Kamaruzzaman et al., 2002; Emeka et al., 2010; Antia et al., 2012). Sorting, skewness, and kurtosis provide insights into transport dynamics and depositional energy (Chakrabarti, 1971; Martins, 2003). Positive skewness often reflects unidirectional flow and competence of the transporting agent, while negative skewness indicates winnowing of fine fractions (Valia & Cameron, 1977; Gujar et al., 2007). Kurtosis variations, in turn, highlight differences in sediment transport processes (Malvarez et al., 2001).

Recent advances in sedimentological studies have demonstrated that grain size distributions, when integrated with hydrodynamic data, can provide robust indicators of sediment provenance, transport pathways, depositional energy conditions, and environmental variability. Consequently, grain size statistics remain one of the most widely applied tools in paleoenvironmental and paleoecological reconstructions.

Recent studies emphasize the importance of tidal asymmetry in sediment deposition. Emeka et al. (2010) demonstrated that both flood and ebb currents actively shape facies in the Calabar and Great-Kwa Rivers, identifying four distinct facies based on grain size parameters. Similarly, Antia et al. (2012) recognized upper and lower facies in the Qua-Iboe River estuary, reflecting changes in mean grain size and sorting along the channel. These findings align with broader facies models in meandering streams, which typically exhibit fining-upward sequences formed by lateral and vertical accretion (Cant & Walker, 1978). Nichols et al. (1991) further proposed a tripartite estuarine facies model, highlighting sand-mud-sand successions controlled by energy gradients.

Despite these advances, significant uncertainties remain regarding the spatial variability of sediment textures within tropical tidal rivers, particularly in regions experiencing increasing anthropogenic modification. Furthermore, the combined influence of tidal asymmetry, channel morphology, and sediment supply on facies architecture has not been fully evaluated in many West African estuarine systems.

Modern tidal channel deposits are notable for their high preservation potential due to rapid sedimentation below the depth of wave reworking (Longhitano *et al*., 2025). Recognition of tidal signatures in fluvial sediments has been advanced by Van den Berg et al. (2007), while Bricker and Troup (1975) emphasized the role of sediment supply, bottom morphology, and

hydrodynamics in facies distribution. More recent work underscores the need to integrate sedimentological perspectives with hydrodynamic modeling to reconstruct paleoenvironmental conditions (Green, 2011; Tessier et al., 2010).

Although previous studies have documented general sedimentological characteristics of the Calabar River and adjacent estuaries (Emeka et al., 2010; Antia et al., 2012), there remains limited understanding of the present-day grain size distribution patterns across the entire tidal channel and how these patterns relate to hydrodynamic conditions and sedimentary facies development. In addition, the implications of these sedimentary characteristics for paleoenvironmental reconstruction under conditions of increasing human disturbance have not been comprehensively investigated. Addressing these knowledge gaps is necessary for improving interpretations of ancient tidal deposits preserved in the geological record.

Given the economic and paleoenvironmental significance of tidal channels, modern systems such as the Calabar River warrant detailed investigation. Recent anthropogenic activities, including dredging, sand mining, and channel modification, have altered the bathymetric configuration and sediment dynamics of the Calabar River. These changes may influence sediment transport pathways, depositional patterns, and facies distribution, thereby necessitating a comprehensive investigation of grain size characteristics and sedimentary architecture within the river system. Accordingly, this study aims to: (i) analyze the relationships between flow characteristics and grain size parameters in the Calabar River estuary and tidal channel; "(ii) delineate and classify sedimentary facies based on grain size characteristics and hydrodynamic conditions to facilitate recognition of their ancient counterparts in the rock record;" and (iii) characterize sedimentary facies to provide insights into depositional processes and paleoenvironmental reconstruction.

The outcomes of this study will provide a modern sedimentological framework for interpreting ancient estuarine and tidal channel deposits. The results will also contribute to improved paleoenvironmental reconstruction, enhance understanding of sediment transport processes in tropical tidal rivers, and provide baseline information for the sustainable management of the Calabar River ecosystem.

1.1 Study Area

1.1.1 Location

The study area comprises segments of the Calabar River, located along the southeastern coast of Nigeria within Cross River State. Geographically, the river lies between 8°14′34″E and 8°20′34″E longitude and 4°53′27″N and 5°03′45″N latitude (Fig. 1). The Calabar River forms part of the Cross River estuarine system and discharges into the Atlantic Ocean through the Cross River estuary. The river represents a transitional environment where fluvial and marine processes interact to control sediment transport and deposition. ***1.1.2 Geology***

The Calabar River, a major tributary of the Cross River, originates from the Oban Hills (Fig. 2). "The geology of the area is dominated by sediments of the Niger Delta and Calabar Flank provinces. The Calabar River traverses unconsolidated Quaternary alluvial deposits, Recent estuarine sediments, and coastal plain sands derived from the Benin Formation. These deposits consist predominantly of sands, silts, clays, and organic-rich sediments that have accumulated under the influence of fluvial, estuarine, and tidal processes."The river channel traverses sedimentary terrains of Tertiary to Recent ages, cutting across coastal plain sands and alluvial deposits. "Previous investigations indicate that sediments within the river channel are predominantly fine- to medium-grained sands interbedded with muddy sediments. Their distribution reflects variations in hydrodynamic energy associated with tidal currents.

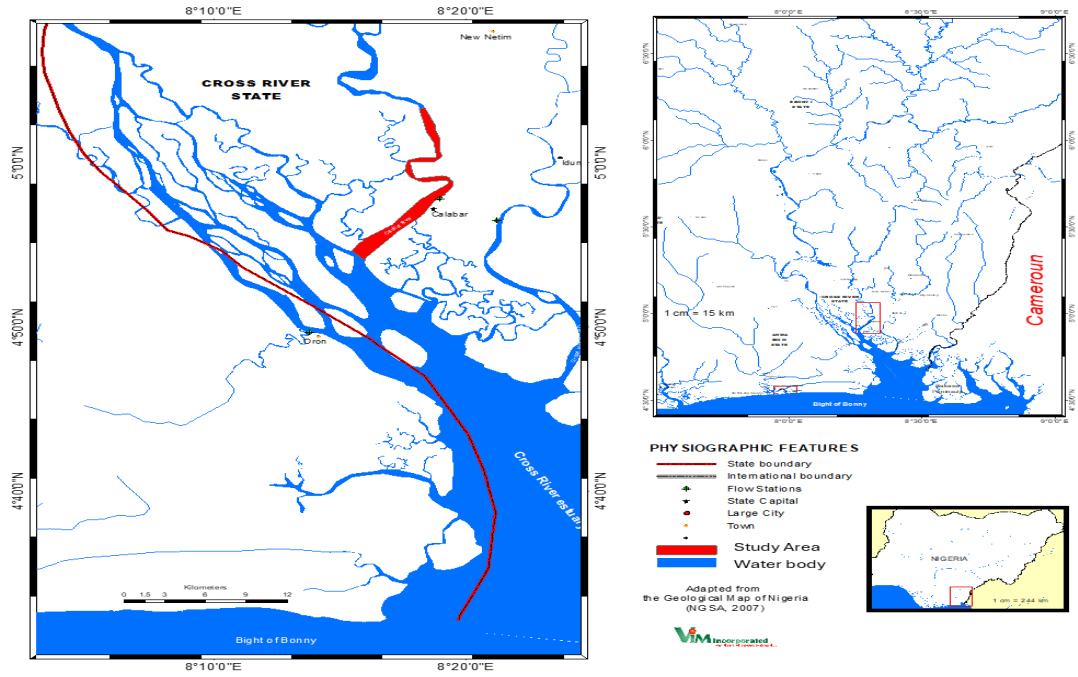

Fig. 1: Study Location Map of Calabar River

discharge, and local channel morphology."

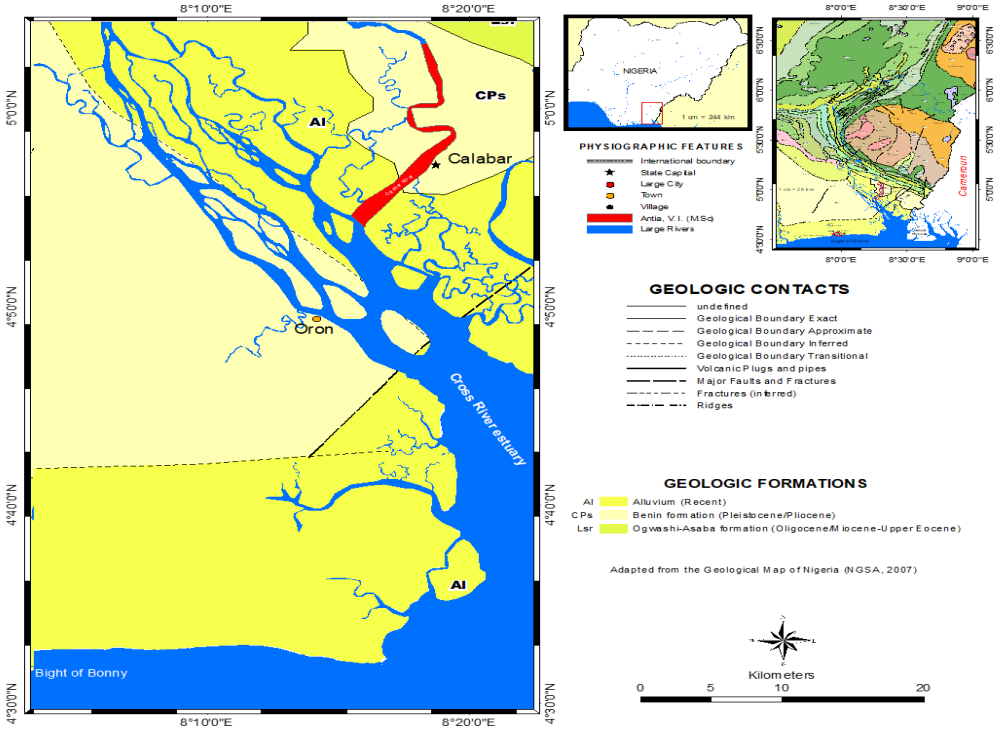

Fig. 2: A geologic map showing study segments of Calabar River (Adapted from Nigerian Geological Survey Agency, 2007)

1.1.3 Climate

The study area lies within the humid equatorial rainforest belt, strongly influenced by southwesterly winds. The climate is characterized by a rainy season from April to October, accounting for nearly 80% of annual rainfall, with peak precipitation in June and July. Mean annual rainfall exceeds 2,000 mm, while temperatures range between 22.5°C and 30°C. Relative humidity is consistently

high, averaging 73–88% throughout the year (Agbiji et al., 2024). Rainfall is highly seasonal, with peak precipitation occurring during the wet season and minimum rainfall during the dry season. (Cross River Climate Data, 2025).

1.1.4 Vegetation

The shorelines of the Calabar River are fringed by mangrove swamps dominated by *Rhizophora* species and invasive *Nypa palms (*Nypa fruticans)**. The western bank is more densely vegetated, while the eastern bank has been modified by industrial activities. Parts of the eastern bank have undergone significant anthropogenic modification resulting from urban development, industrial activities, and port operations. Vegetation plays a crucial role in sediment stabilization, tidal channel morphology, and ecological balance.

1.1.5 Geomorphological Setting

The Calabar River, situated within a meso-tidal regime (Antia et al., 2012), is characterized by alternating flood and ebb currents that actively shape sedimentary processes. Sands are typically deposited during peak flood and ebb stages, while mud accumulates during slack water when current velocities diminish (Mead & Moores, 2005). The river channel exhibits spatial variations in bathymetry and sediment texture resulting from changing hydrodynamic conditions along the tidal gradient." (Debekeme et al., 2022).

The distribution of sedimentary facies is strongly influenced by channel depth, meandering geometry, and hydrodynamic energy gradients, which together control depositional variability. The geomorphology of the river is characterized by tidal flats, point bars, channel margins, and subtidal channels. The distribution of these depositional environments reflects variations in tidal energy, sediment supply, and channel morphology. These facies are shaped not only by natural tidal currents but also by anthropogenic disturbances such as dredging and sand mining, which have altered sedimentary dynamics and channel morphology (Okon et al., 2025). This geomorphological framework underscores the Calabar River's role as a dynamic sedimentary system, where tidal asymmetry, hydrodynamic energy, and human activities interact to produce complex facies architectures with significant implications for paleoenvironmental reconstruction. "The combination of tidal influence, active sediment transport, diverse depositional environments, and increasing anthropogenic modification makes the Calabar River an ideal natural laboratory for investigating grain size distribution patterns and their implications for paleoenvironmental reconstruction."

2.0 Materials and Methods

Field investigations, including tidal current measurements, bathymetric surveys, and sediment sampling, were conducted in September 2011 during representative spring, mean, and neap tidal conditions.

The study employed a combination of field measurements and laboratory analyses to investigate tidal currents, bathymetry and sediment characteristics in the Calabar River. A buoyant float constructed from a sealed plastic container was used as the drifting object. The drift distance was measured using a survey tape, and a minimum of three replicate measurements were obtained at each observation period. Measurements were conducted during both flood and ebb tidal phases.

2.1 Field Procedures

2.1.1 Tidal Current Measurement

Surface tidal current velocities were measured at Adiabo Bridge and Marina Beach during spring, mean, and neap tidal phases. The Lagrangian method was adopted, whereby a float was released at mid-channel and the time taken to drift across a pre-measured distance was recorded using a stopwatch. Measurements were repeated at 15-minute intervals over 12-hour cycles to capture both flood and ebb phases. Current velocity was calculated as the ratio of distance travelled to time elapsed.Near-

bottom current velocities were estimated using an empirical reduction factor of 0.7 applied to measured surface velocities, following the approach adopted by Emeka et al. (2010) for tidal channels within southeastern Nigeria.

2.1.2 Depth Sounding

Bathymetric data were acquired using an echo-sounder mounted on an outboard motor boat. Geographic coordinates and distances between sounding points were recorded with a Global Positioning System (GPS). Depth values were later contoured to generate bathymetric maps of the river channel. Soundings were acquired along predetermined survey tracks oriented parallel to the river channel. Data points were collected at regular intervals to ensure adequate spatial coverage of the study area.

2.1.3 Sediment Sampling

Sediment samples (n = 50) were collected using a Van Veen grab sampler along ten cross-channel transects spaced at 2.4 km intervals, with three stations per transect (Fig. 3). Sampling depths ranged between 1–20 m. Coordinates were recorded with GPS, and depth soundings were taken at each station. Samples were stored in labelled polythene bags for laboratory analysis. The sampling design was intended to capture spatial variations in sediment characteristics along both longitudinal and transverse gradients within the tidal channel.

2.3 Laboratory Procedures

2.3.1 Bathymetric Map Analysis

Depth values were corrected relative to Mean Tide Low Water (MTLW). Contoured bathymetric maps were produced, and three cross-sectional profiles were extracted to illustrate channel morphology.

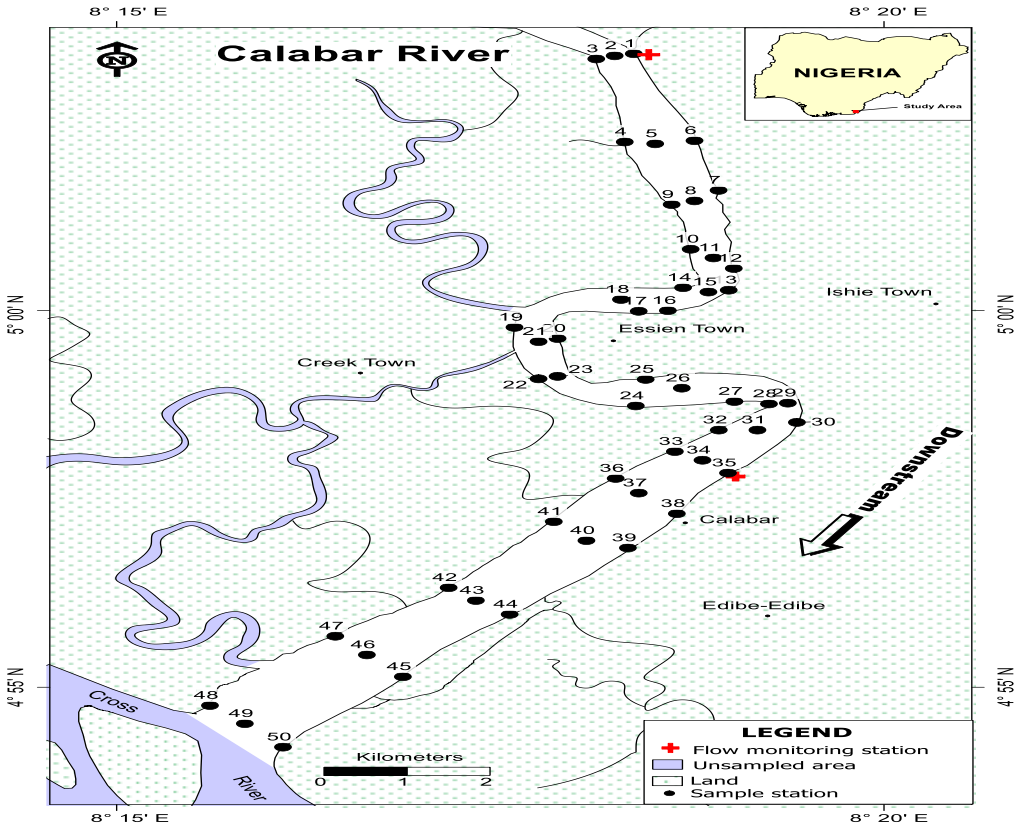

Fig. 3: Distribution of sediment sampling stations and bathymetric survey locations along the Calabar River.

2.3.2 Grain Size Analysis

Sediment samples were oven-dried at 105°C for 24 h until constant weight was achieved. . Lumps were disaggregated using a porcelain mortar and pestle. Subsamples (100–250 g) were sieved at 0.5φ intervals using a Ro-Tap mechanical shaker for 10 minutes. Sieves ranged from −1ϕ to 4ϕ at 0.5ϕ intervals, encompassing gravel, sand, and fine sediment fractions.

Residues retained on each sieve were weighed, and percentages of sediment fractions were calculated. Grain size statistical parameters (mean, sorting, skewness, kurtosis) were derived from cumulative frequency curves using the Folk and Ward (1957) formula:

Mean (M_z) = $\frac{\emptyset 16+\emptyset 50+\emptyset 84}{3}$ (1)

Sorting (D) $\sigma_1 = \frac{\emptyset_{84}-\emptyset_{16}}{4} + \frac{\emptyset_{95}-\emptyset_5}{6.6}$ (2)Skewness (SK_I) = $\frac{\emptyset 16+\emptyset 84-2(\emptyset 50)}{2(\emptyset 84-\emptyset 16)} + \frac{\emptyset 5+\emptyset 95-2(\emptyset 50)}{\emptyset_{95}-\emptyset_5}$ (3)

Kurtosis (K_G) $\frac{\emptyset 95-\emptyset 5}{2.44(\emptyset 75-\emptyset 25)}$ (4)

Grain size parameters were calculated from cumulative frequency distributions following Folk and Ward (1957) using Microsoft Excel spreadsheets.

2.5 Statistical Analysis

Descriptive statistics were employed to summarize grain-size parameters. Spatial trends in sediment texture were evaluated through comparisons of mean grain size, sorting, skewness, and kurtosis among sampling locations. Frequency distribution curves and cumulative probability plots were used to identify sediment populations and infer depositional processes.

3.0 Results and Discussion

3.1 Results

3.1.1 Hydrodynamics

The Calabar River exists within a meso-tidal setting and is characterized by semi-diurnal tides. The channel is defined by two tidal regimes: flood and ebb tides. A standstill in water level, known as slack water, occurs at the end of both flood and ebb stages. High slack water is observed at the end of a flood tide, while low slack water occurs at the end of an ebb tide.

Surface and near-bottom current velocity profiles are presented in Fig. 4 and 5, with maximum velocities during spring, mean, and neap tides shown in Tables 1 and 2. Maximum surface velocities ranged from 0.41–0.61 m/s at Adiabo Bridge and 0.65–0.95 m/s at Marina Beach, with spring tides consistently exhibiting the highest velocities. The time–velocity asymmetry of the observed flow indicates ebb dominance across both tidal channels. In addition to tidal currents, factors such as discharge from smaller rivers and fluvial energy input from rainfall contribute to this ebb dominance.

3.1.2 Bathymetry

The Calabar River is a NE–SW trending tidal river with a meandering channel pattern. Channel depth increased from approximately 2 m along the margins to a maximum of 20 m within the central thalweg. The studied segment covers a surface area of 17.45 km² and a total length of 24 km. Channel depths range from 2 to 20 m, with the eastern banks generally deeper than the western banks. The complex bathymetry of the river is partly attributed to its dredging history.

The bathymetric map (Fig. 6a) shows the deepest part of the channel (20 m) located centrally. Cross-sectional profiles (Fig. 6b) reveal increasing depth toward the mid-channel, highlighting the asymmetry of channel morphology.

4.*1.4 Sediment*

Grain Size Classes of Bottom Sediment

Sand fractions dominate the channel, whereas mud and gravel occur as localized patches. Fine- and medium-grained sands constitute the most abundant sediment classes, while gravel is restricted to isolated high-energy zones within the central channel.

Mud: Upstream sediments contain 10–30% mud, while central portions are generally low (0–10%), with isolated patches of 20–30%. Downstream sediments range from 0–30%, with localized areas reaching 30–40% along

the eastern flank (Fig. 9). Sand and muddy sand collectively account for over 80% of sampled sediments.

Very Fine Sand: Upstream sediments contain 10–20%, with central patches exceeding 50%. Downstream sediments are dominated by 20–30% fractions (Fig. 10).

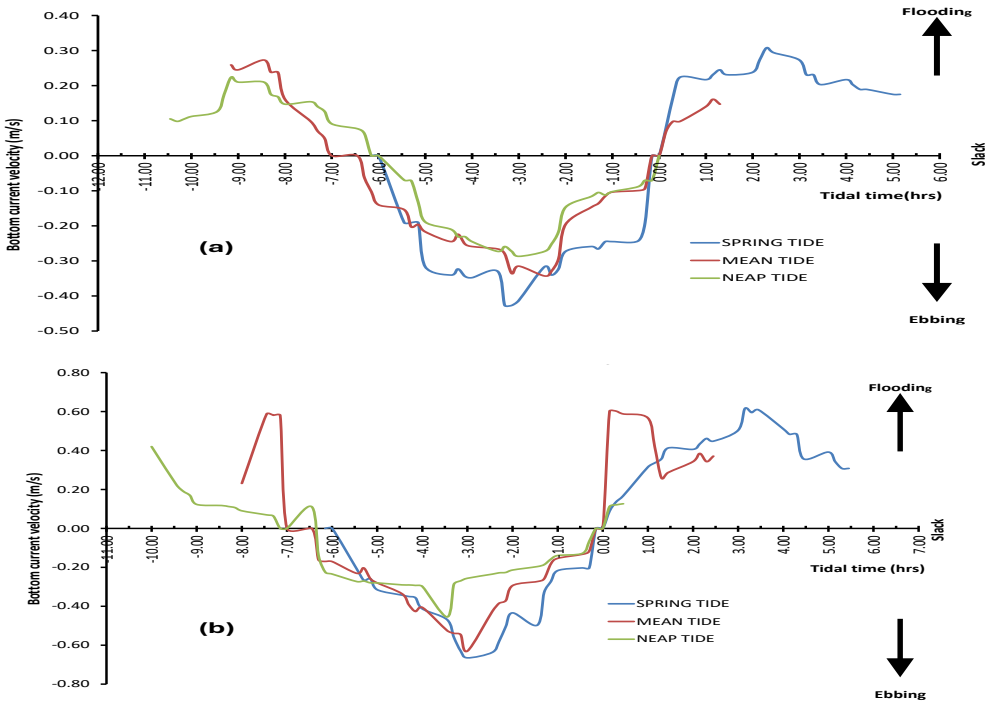

Fig. 5: Near bottom current velocity profiles for (a) Spring Mean and Neap at Adiabo Bridge, Calabar River and (b) Spring, Mean and Neap at Marina Beach, Calabar River

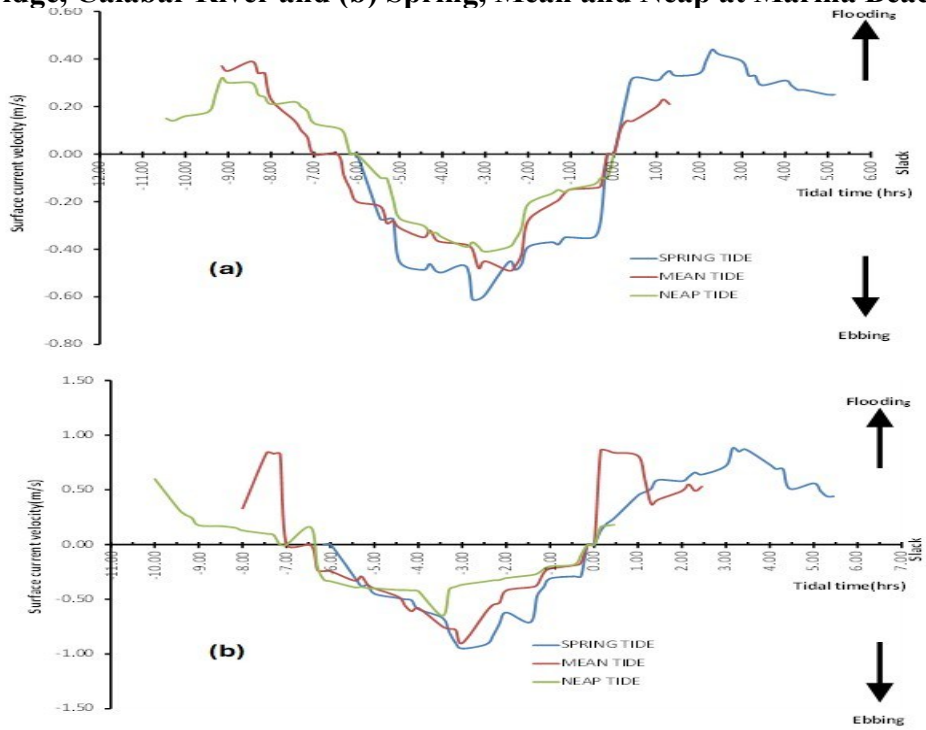

Fig. 4: Tidal current velocity profiles for Calabar River (a) spring, mean, and neap at Adiabo Bridge and (b) Spring, Mean, and Neap at Marina Beach

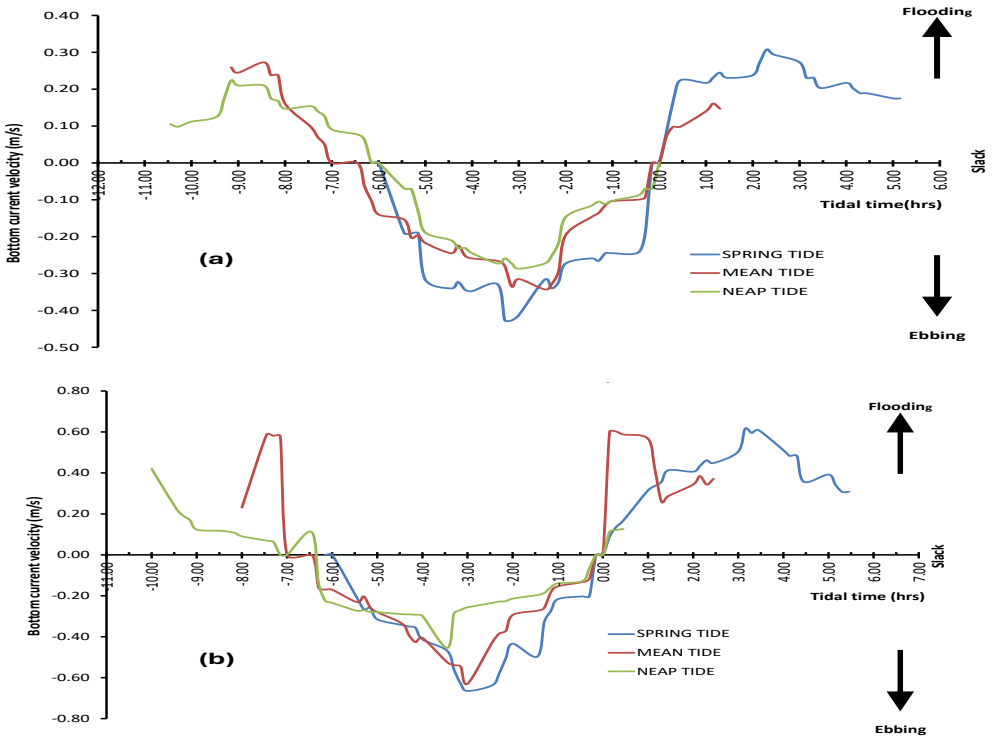

Fig. 5: Near bottom current velocity profiles for (a) Spring Mean and Neap at Adiabo Bridge, Calabar River and (b) Spring, Mean and Neap at Marina Beach, Calabar River

Table 1: Maximum Surface Tidal Current Velocities (m/s) in the Calabar River during Spring, Mean, and Neap Tides

Tidal Cycle	Adiabo Bridge (m/s)	Marina Beach (m/s)
Spring	0.61	0.95
Mean	0.49	0.90
Neap	0.41	0.65

Table 2: Maximum Bottom Tidal Current Velocities (m/s) in the Calabar River during Spring, Mean, and Neap Tides

Tidal Cycle	Adiabo Bridge (m/s)	Marina Beach (m/s)
Spring	0.43	0.67
Mean	0.34	0.63
Neap	0.27	0.46

Fine Sand: Upstream sediments comprise 10–20%, with central patches reaching 50%. Downstream sediments are generally 10–20%, while the mouth is nearly devoid of fine sand (Fig. 11).

Medium Sand: Predominantly 10–20% across the channel, with localized patches exceeding 40% near the mouth (Fig.12).

Coarse Sand: Upstream sediments contain 10–30%, while central portions range from 20–60%. Downstream sediments are mainly 10–30% (Fig. 13).

Very Coarse Sand: Sparse upstream (0–10%), with localized 10–20% fractions along the western bank. Central and downstream portions contain 10–20%, with patches exceeding 20% (Fig/ 14).

Gravel: Generally 0–10% across the channel, with isolated central patches reaching 40–60% (Fig. 15).

Textural Classes of Bottom Sediments

Ternary plots modeled after Folk (1980) (Fig. 16–17) reveal that most sediments are classified as sand and muddy sand. Station 26 uniquely contains gravel. Upstream portions are dominated by sand and muddy sand, with localized gravelly mud. Central portions show a mosaic of sand, muddy sand, gravelly mud, gravelly sand, and muddy gravel. Downstream portions are characterized by

muddy sand interspersed with large patches of sand.

Grain Size Statistical Parameters

Sediments portray a predominantly bimodal distribution pattern.

Mean: Upstream sediments are dominated by fine sands, central portions by medium sands, and downstream portions by medium sands with patches of fine sands (Fig. 18).

Sorting: The channel is largely poorly sorted, with central portions showing patches of extremely poorly sorted and moderately sorted sands. Downstream limits contain small patches of moderately sorted sands (Fig. 19).

Skewness: Upstream sediments are near symmetric, with localized positive and negative skewness. Central portions contain mixed skewness types, while downstream sediments are mainly near symmetric with patches of positive and negative skewness (Fig. 20).

Kurtosis: Upstream sediments are predominantly platykurtic, with localized mesokurtic sands. Central portions contain platykurtic sands with patches of mesokurtic and leptokurtic sediments. Downstream sediments are largely platykurtic, with extensive areas of very platykurtic sands (Fig/ 21).

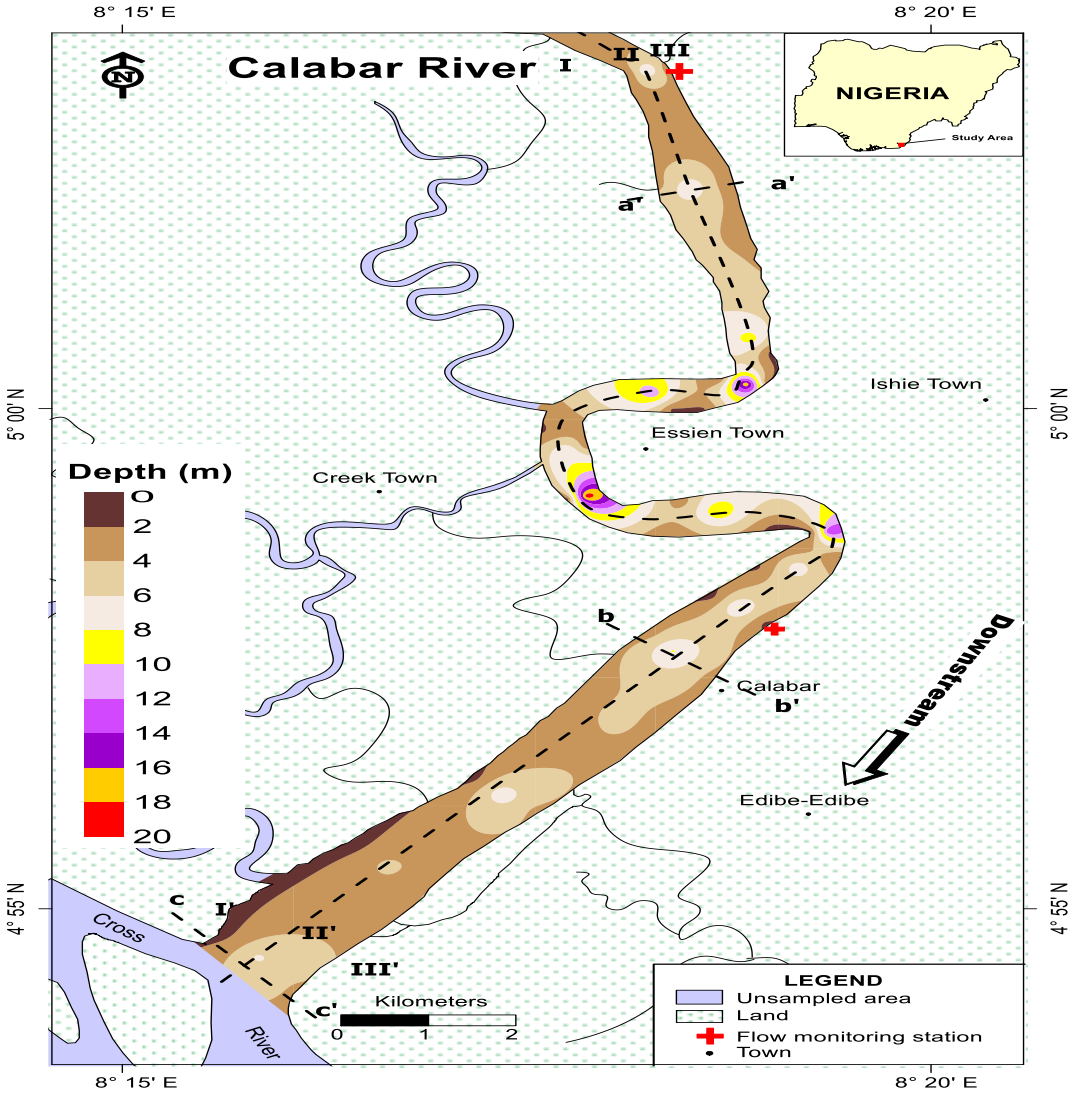

Fig/ 6a:Bathymetry map of Calabar River study segment

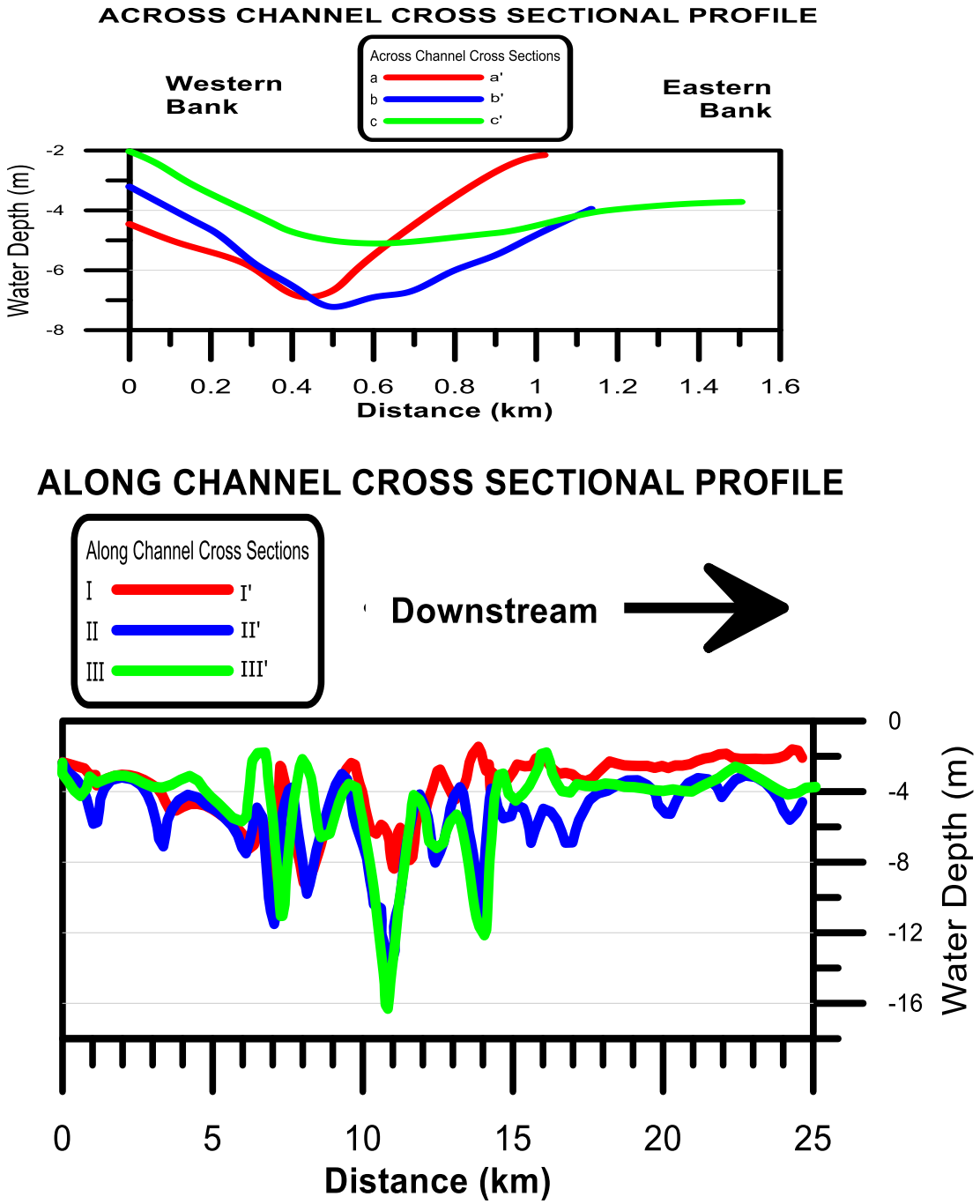

Fig. 6b: Bathymetric cross-sectional profiles of Calabar River study location

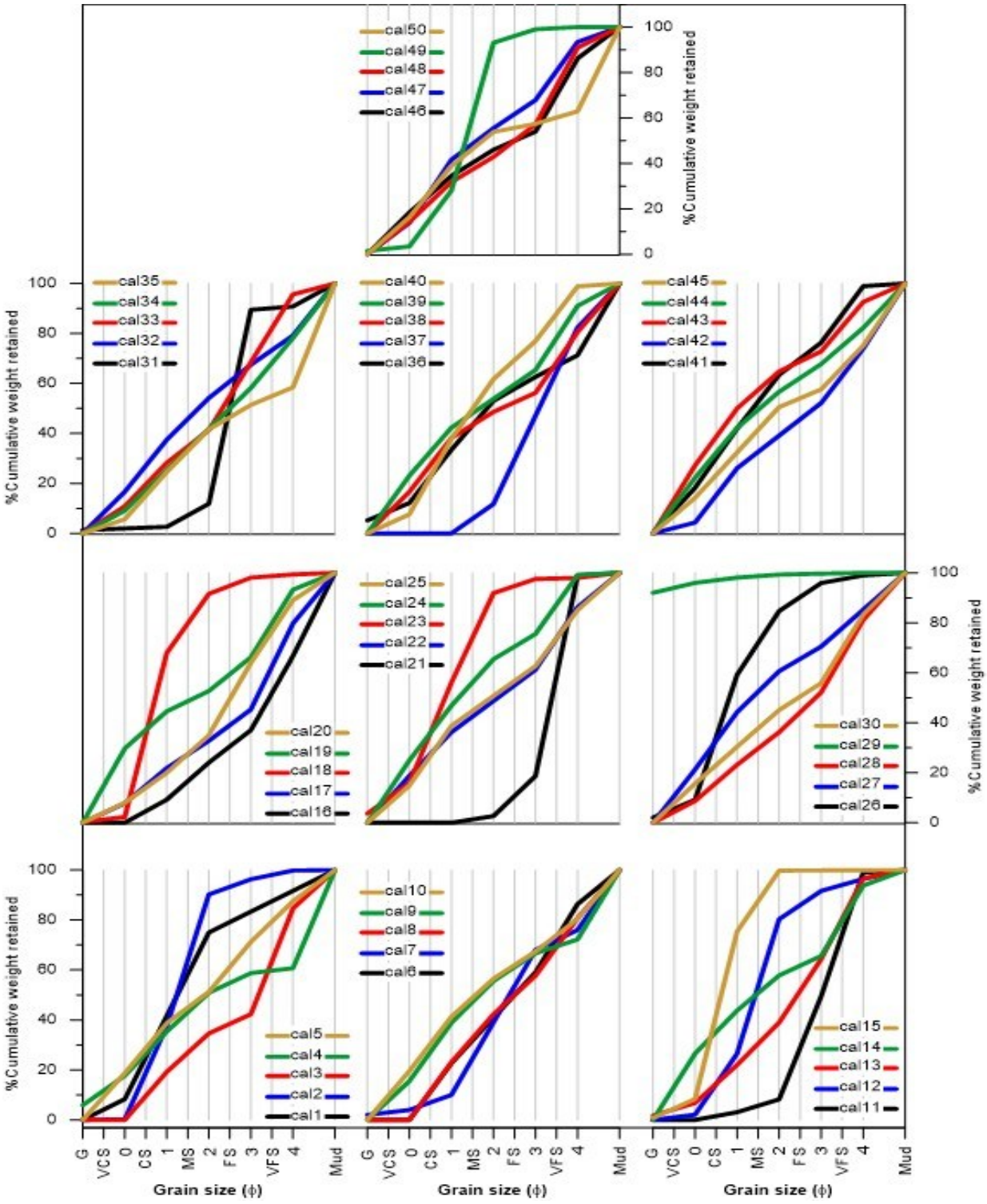

Fig.7: Cummulative frequency curves of Calabar River sediments from stations 1 to 50 (G = gravels, VCS = very coarse sand, CS = coarse sand, MS = medium sand, FS = fine sand, VFS = very fine sand)

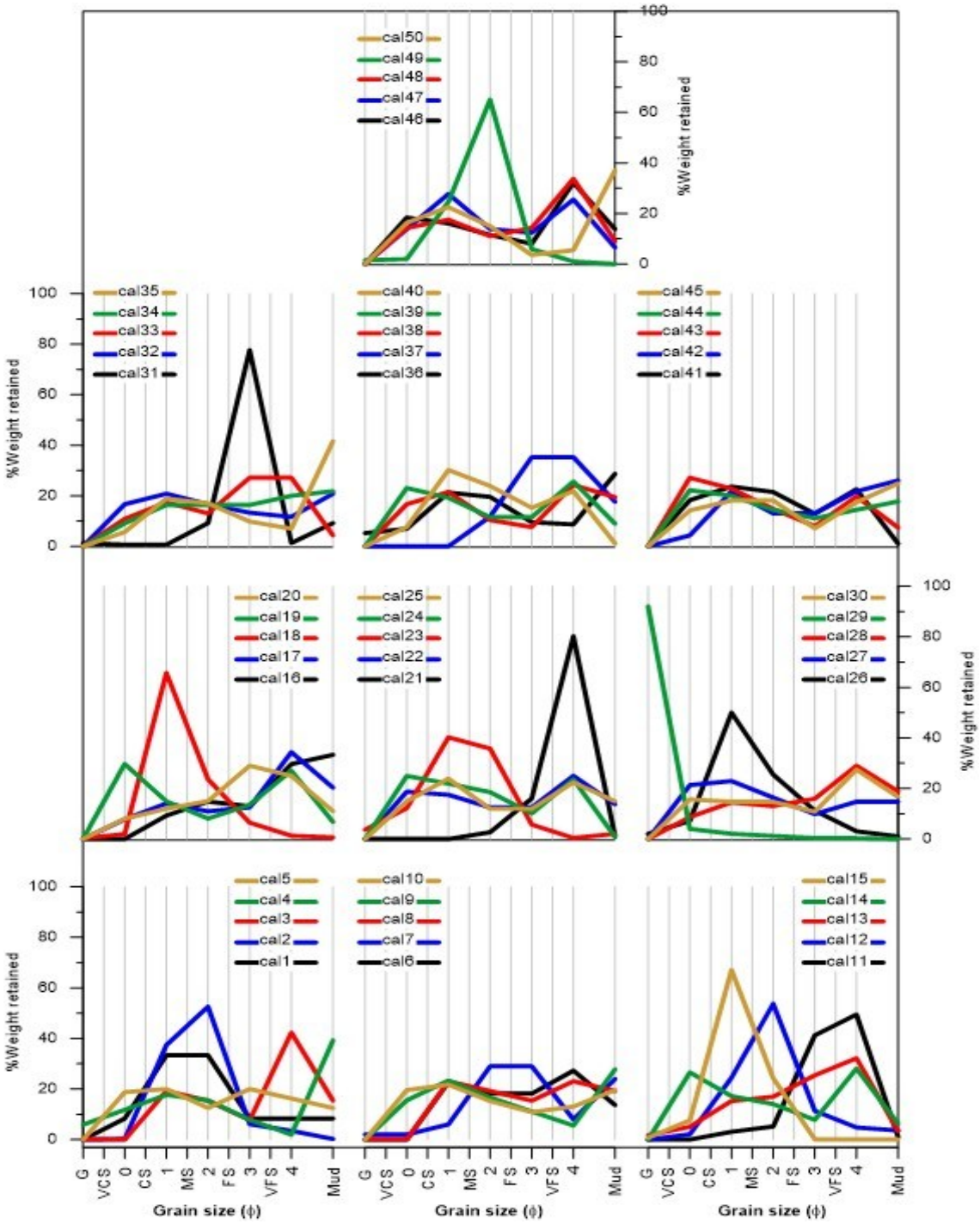

Fig. 8: Weight frequency curves of Calabar River sediments from stations 1 to 50 (G = gravels, VCS = very coarse sand, CS = coarse sand, MS = medium sand, FS = fine sand, VFS = very fine sand)

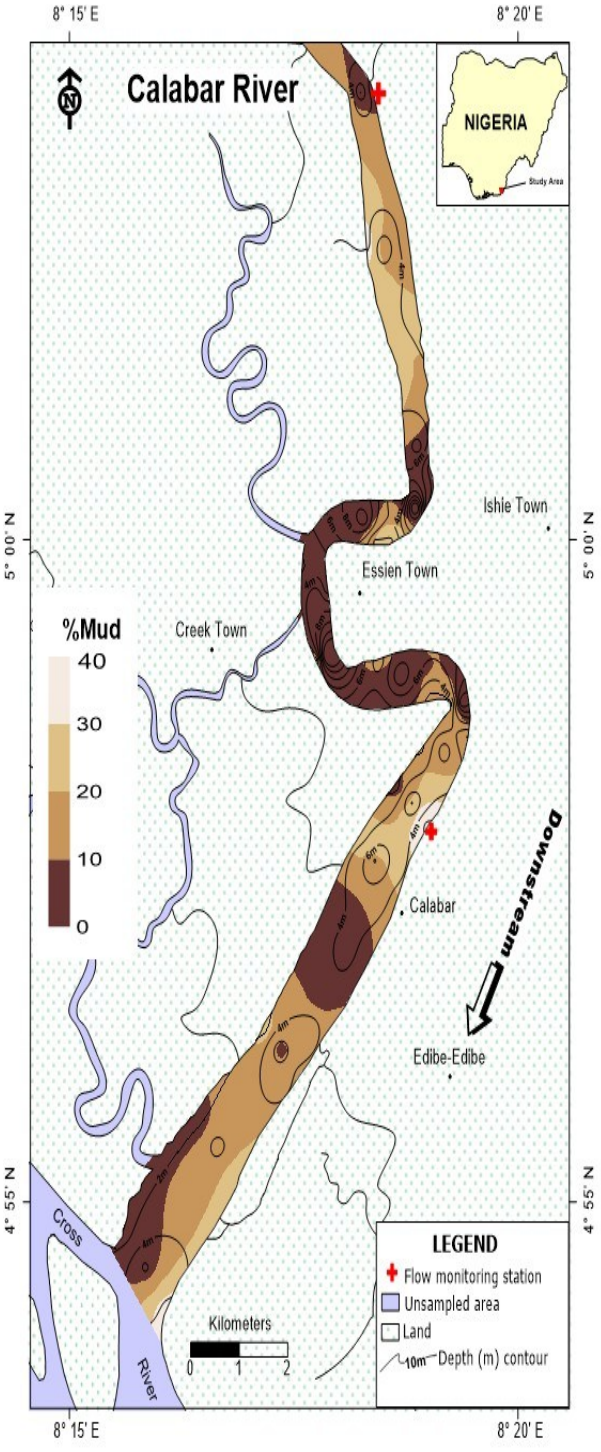

Fig. 9: Distribution of mud in bottom sediment of Calabar River

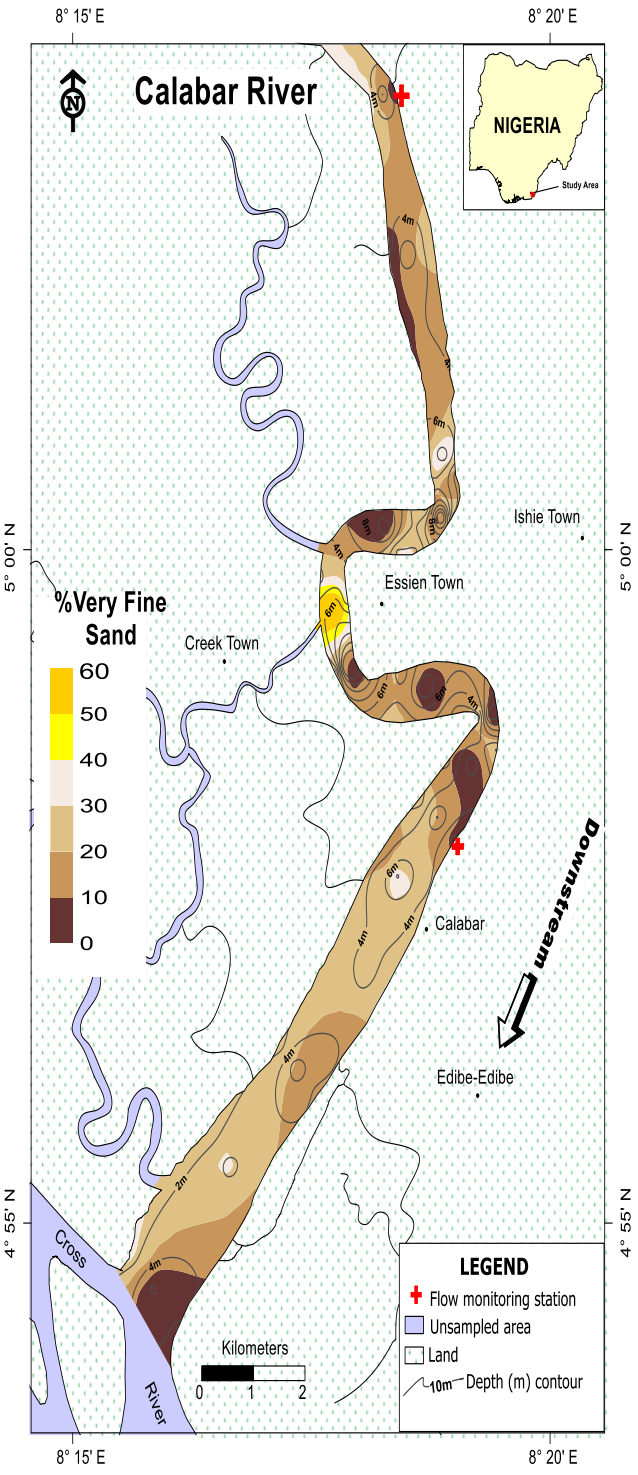

Fig. 10: Distribution of very fine sand in bottom sediment of Calabar River

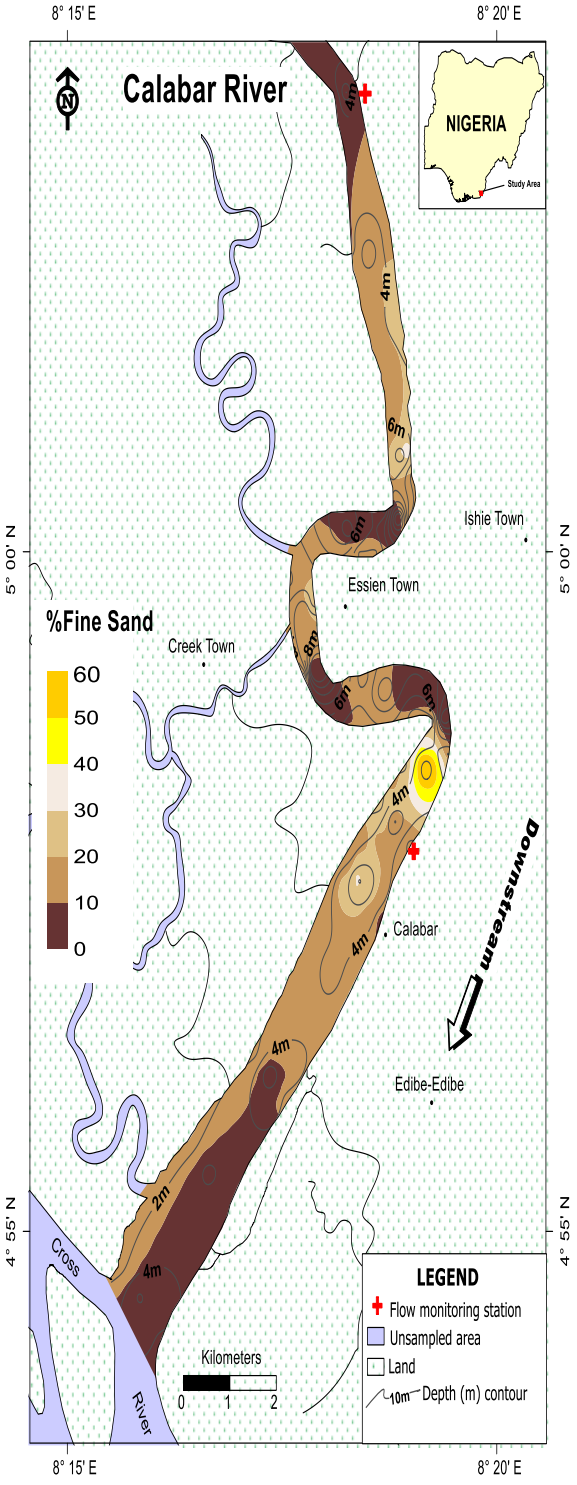

Fig. 11:Distribution of fine sand in bottom sediment of Calabar River

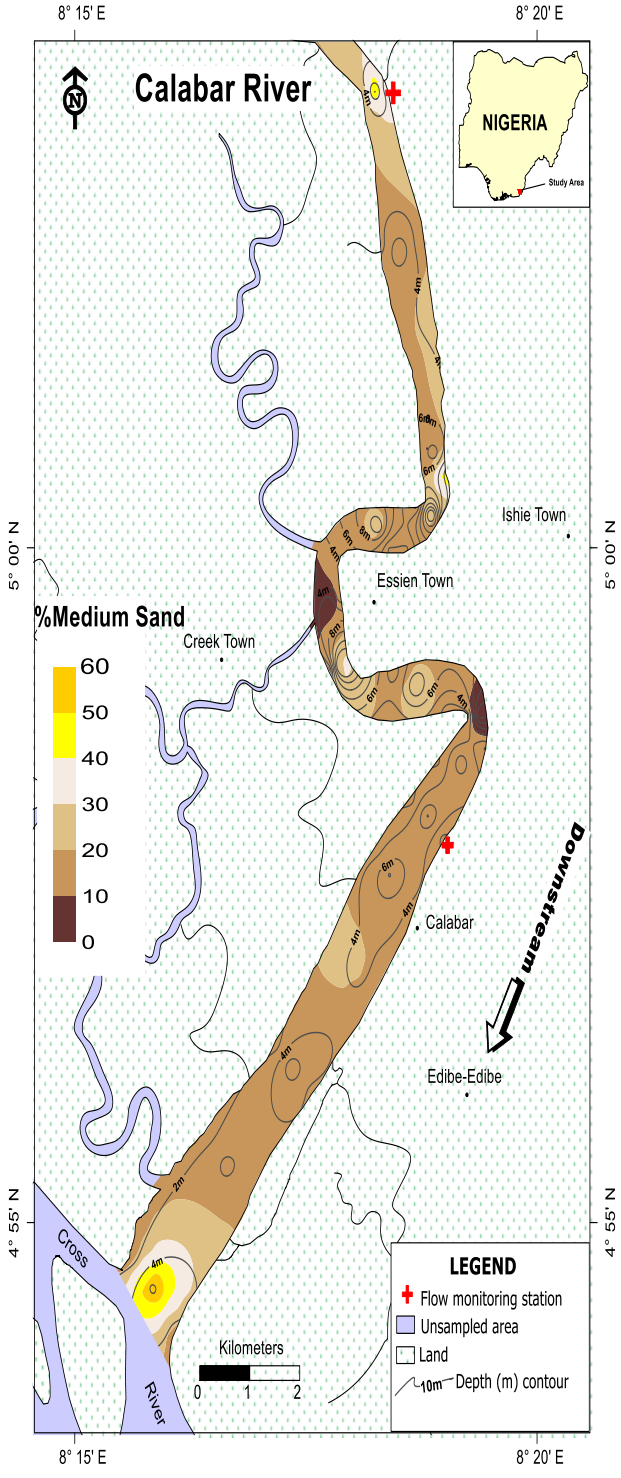

Fig. 12: Distribution of medium sand in bottom sediment of Calabar River

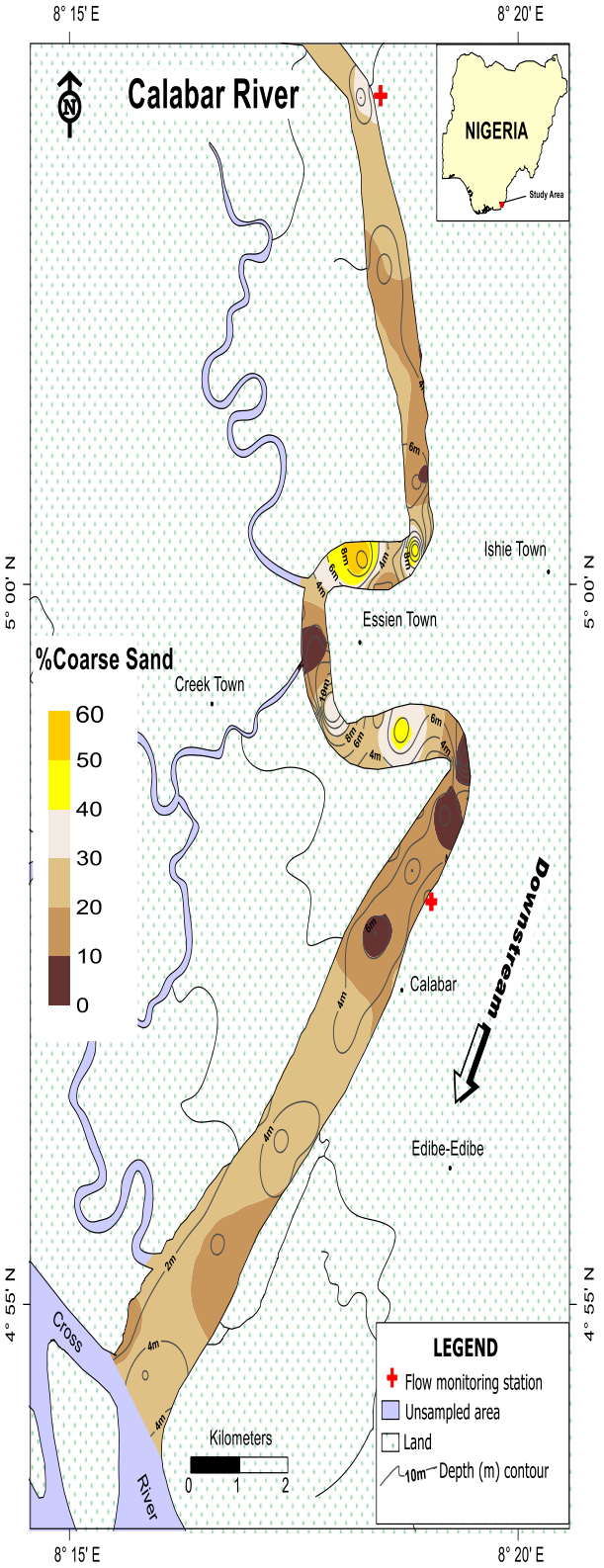

Fig. 13: Distribution of coarse sand in bottom sediment of Calabar River

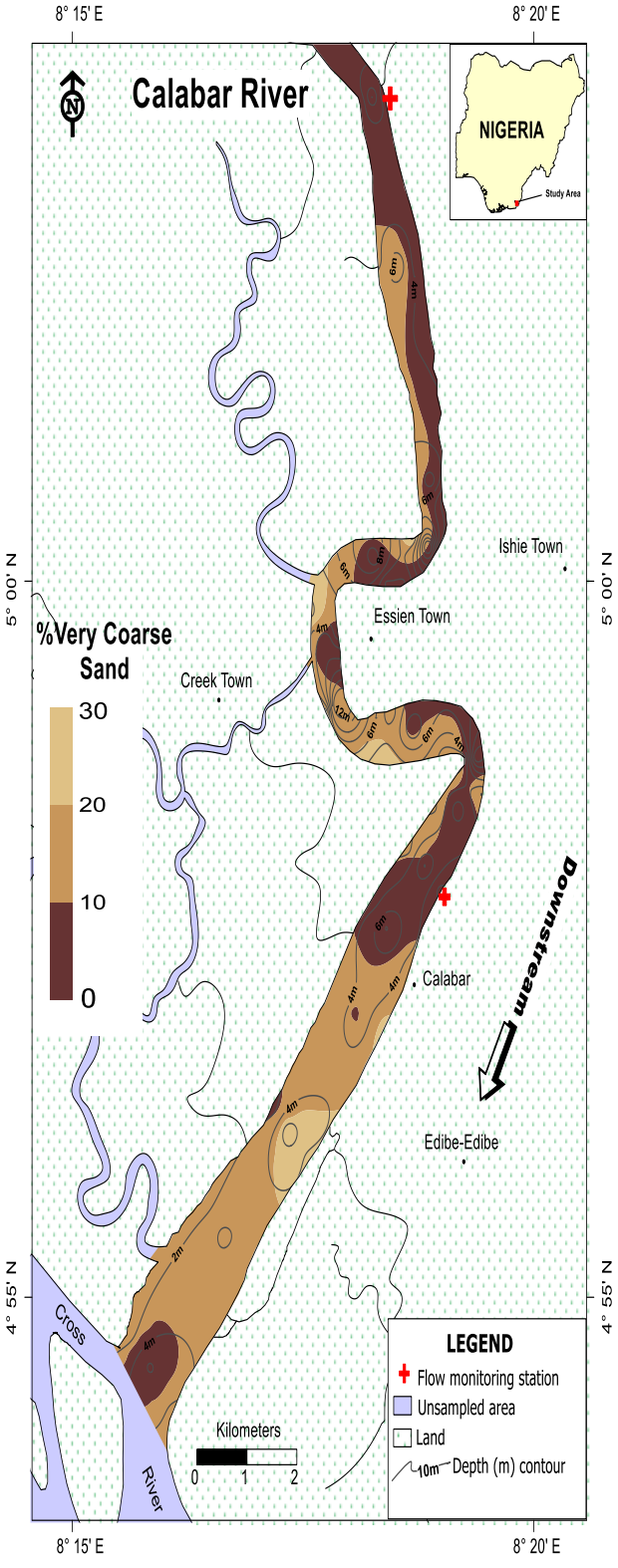

Fig. 14:Distribution of very coarse sand in bottom sediment of Calabar River

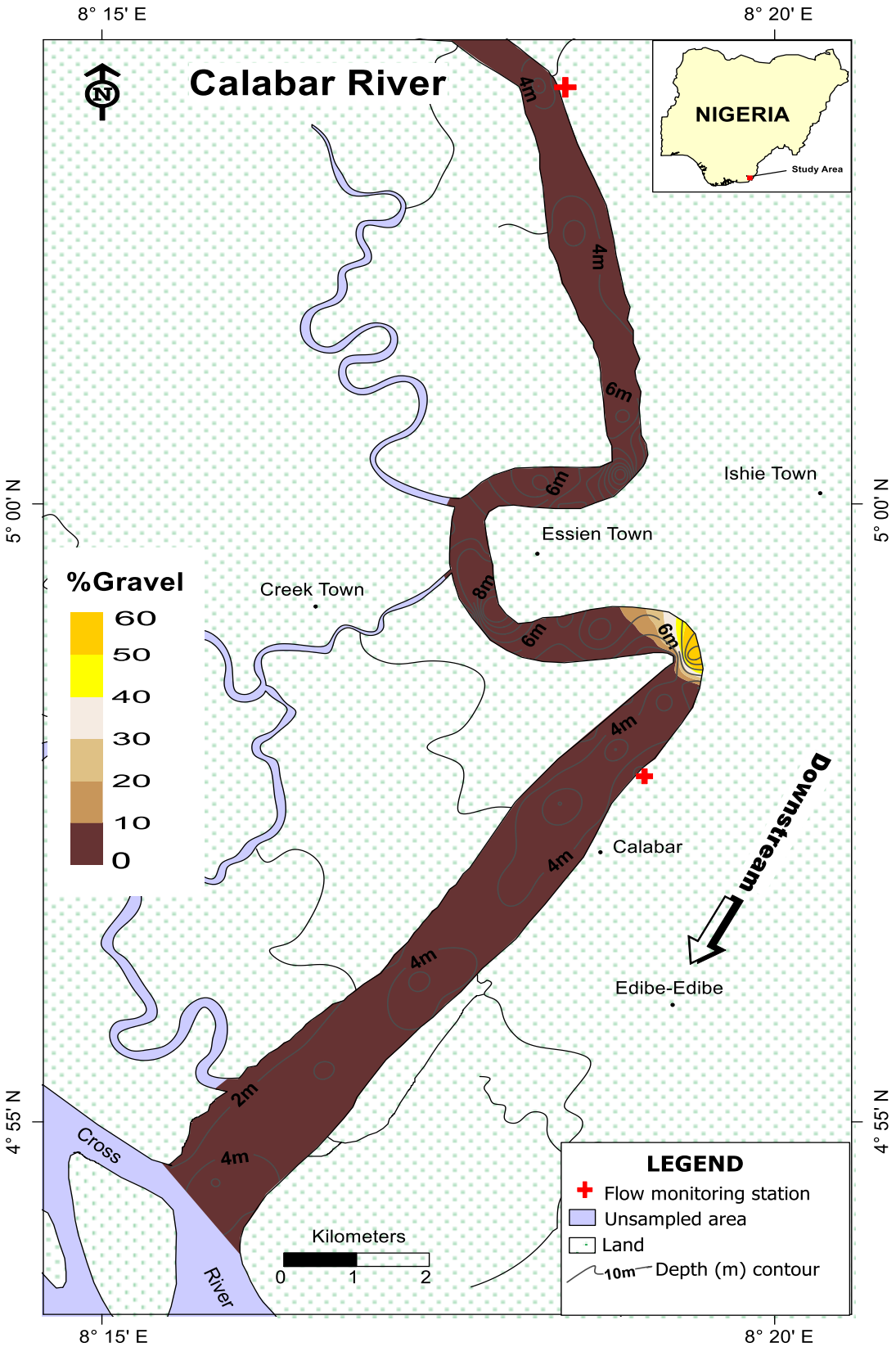

Fig. 15:Distribution of gravel in bottom sediment of Calabar River

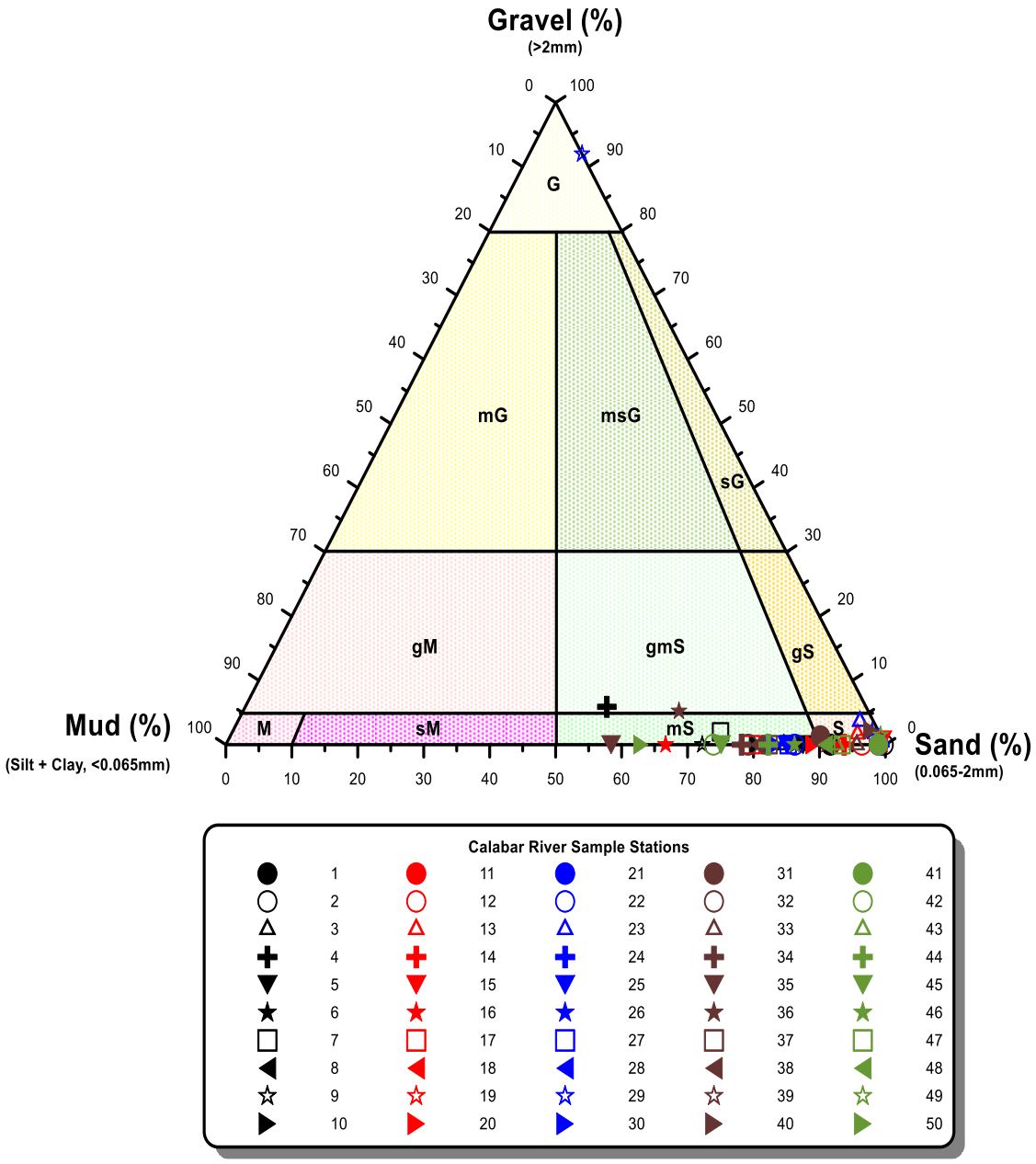

Fig. 16: Ternary diagram of textural classes of Calabar River bottom sediments; G= gravel, mG=muddy gravel, msG=muddy sandy gravel, sG=sandy gravel, gS=gravelly sand, gmS=gravelly muddy sand, gM=gravelly mud, S=sand, mS=muddy sand, sM=sandy mud, M=mud (Modelled after Folk, 1980)

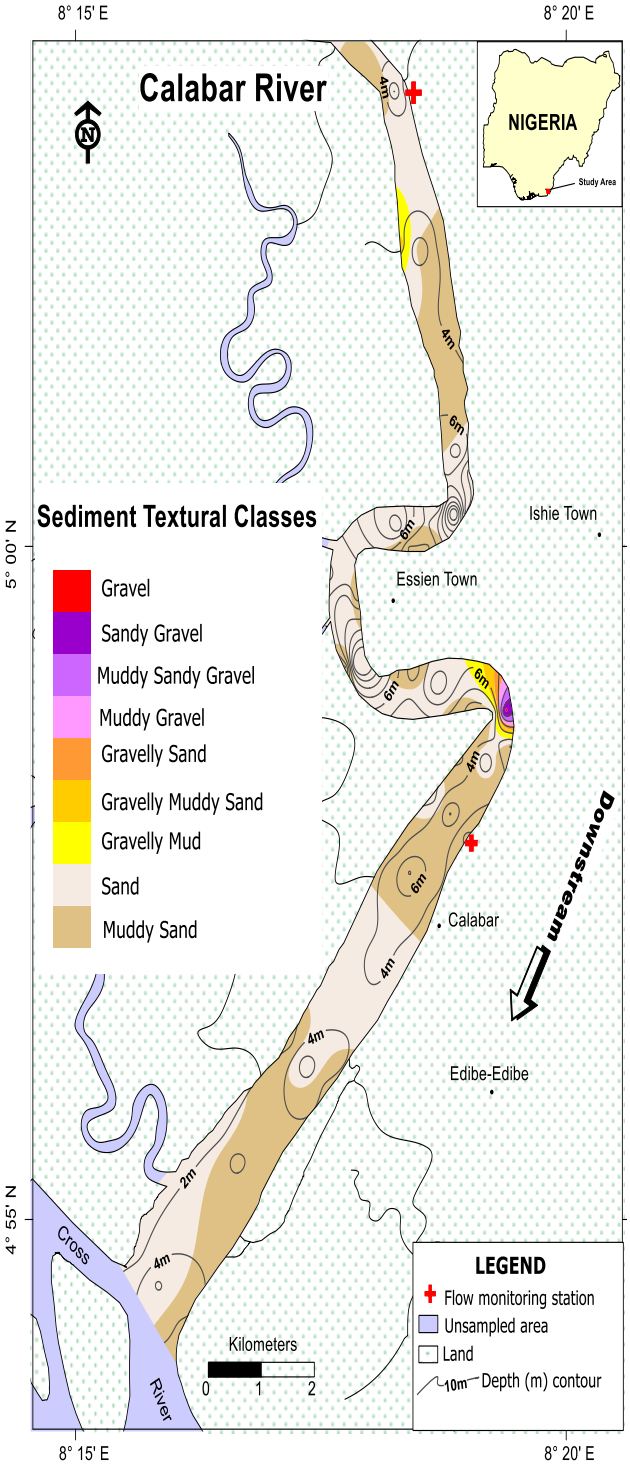

Fig. 17: Distribution of textural classes of Calabar River bottom sediments (Computed from Folk, 1980 ternary diagram)

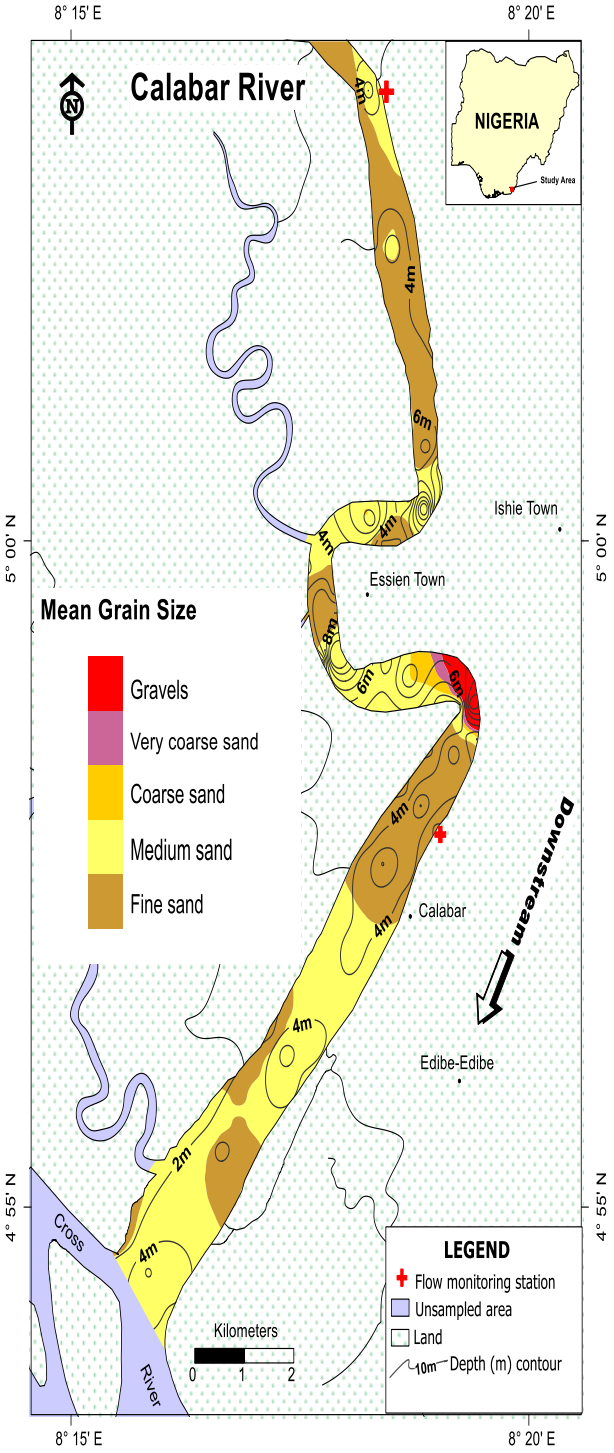

Fig.. 18:Distribution of mean grain size of bottom sediment of Calabar River

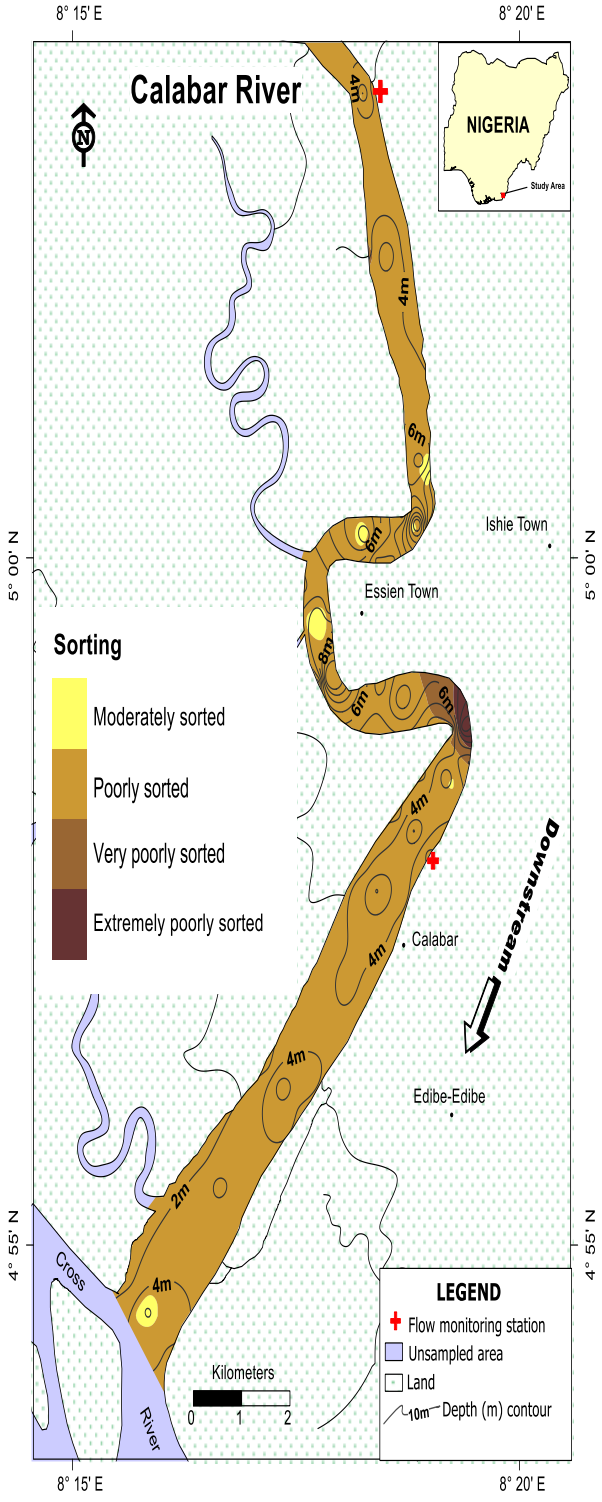

Fig. 19:Distribution of sorting of Calabar River bottom sediment

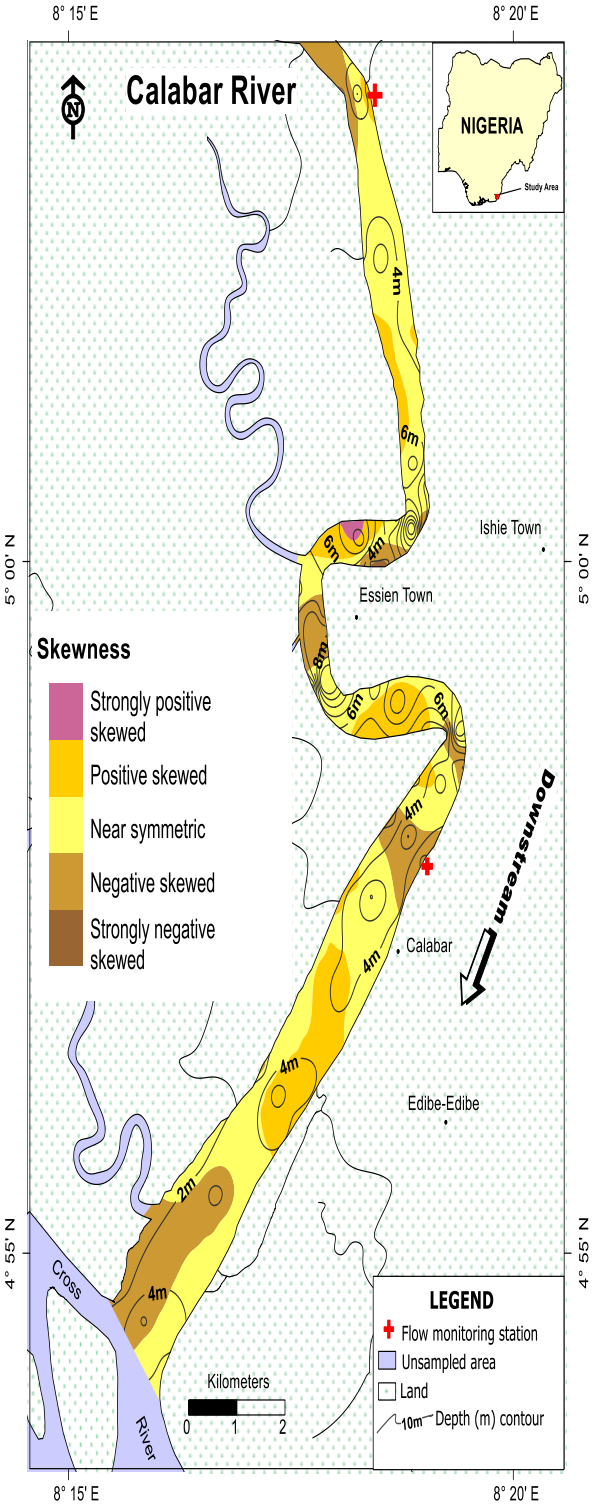

Fig. 20: Distribution of skewness of Calabar River bottom sediment

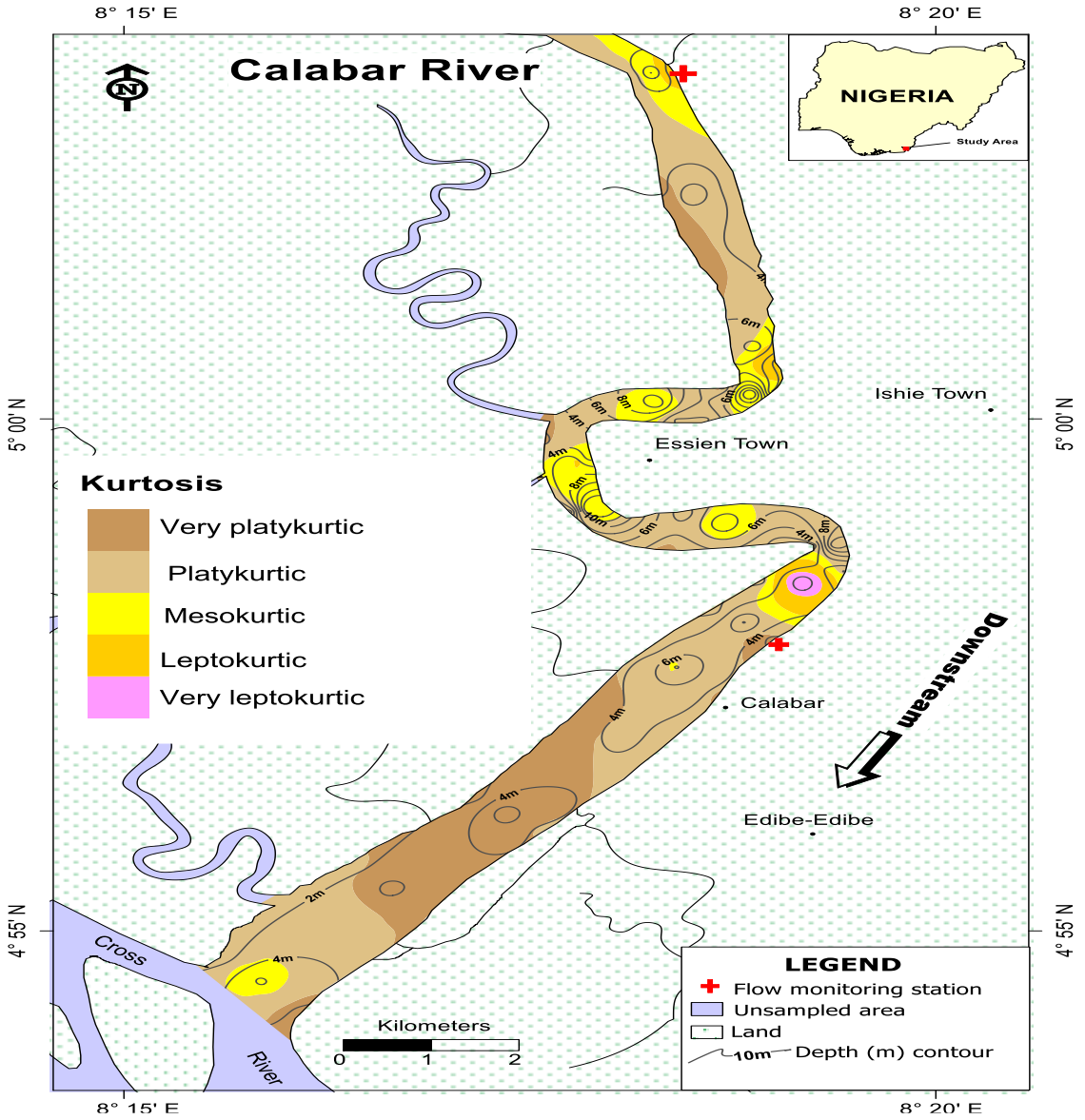

Fig. 21: Distribution of kurtosis of Calabar River bottom sediment

3.1.4 Statistical Cross-Sectional Profiles

Cross-sectional profiles (Figs 22–23) highlight spatial trends:

Mean Grain Size: Decreases toward the banks in upstream and downstream segments, with downstream coarsening along the channel.

Sorting: Improves toward the mid-channel in upstream and central segments but deteriorates at the banks. Downstream profiles show deterioration in sorting.

Skewness: Transitions from near symmetric to negative skewed sediments toward the mid-channel upstream and centrally, while downstream profiles show negative skewness increasing westward.

Kurtosis: Sediments trend from platykurtic at the banks to leptokurtic in the main channel, with downstream profiles becoming increasingly platykurtic.

Lithofacies

Three lithofacies were delineated based on grain size parameters (Fig. 24):

Facies A (Upstream): Extends 6 km, with depths up to 10 m. Texturally fine-grained

sands and muddy sands, poorly sorted, near symmetric, and platykurtic.

Facies B (Central): Extends 8 km, with depths up to 20 m. Medium-grained sands dominate, with patches of fine, coarse, and gravelly sands. Poorly sorted, near symmetric, with mixed skewness and platykurtic to mesokurtic sands.

Facies C (Downstream): Extends 10 km to the mouth, with depths up to 8 m. Medium-grained sands dominate, with patches of fine sands. Poorly sorted, near symmetric, with mixed skewness and predominantly platykurtic sands.

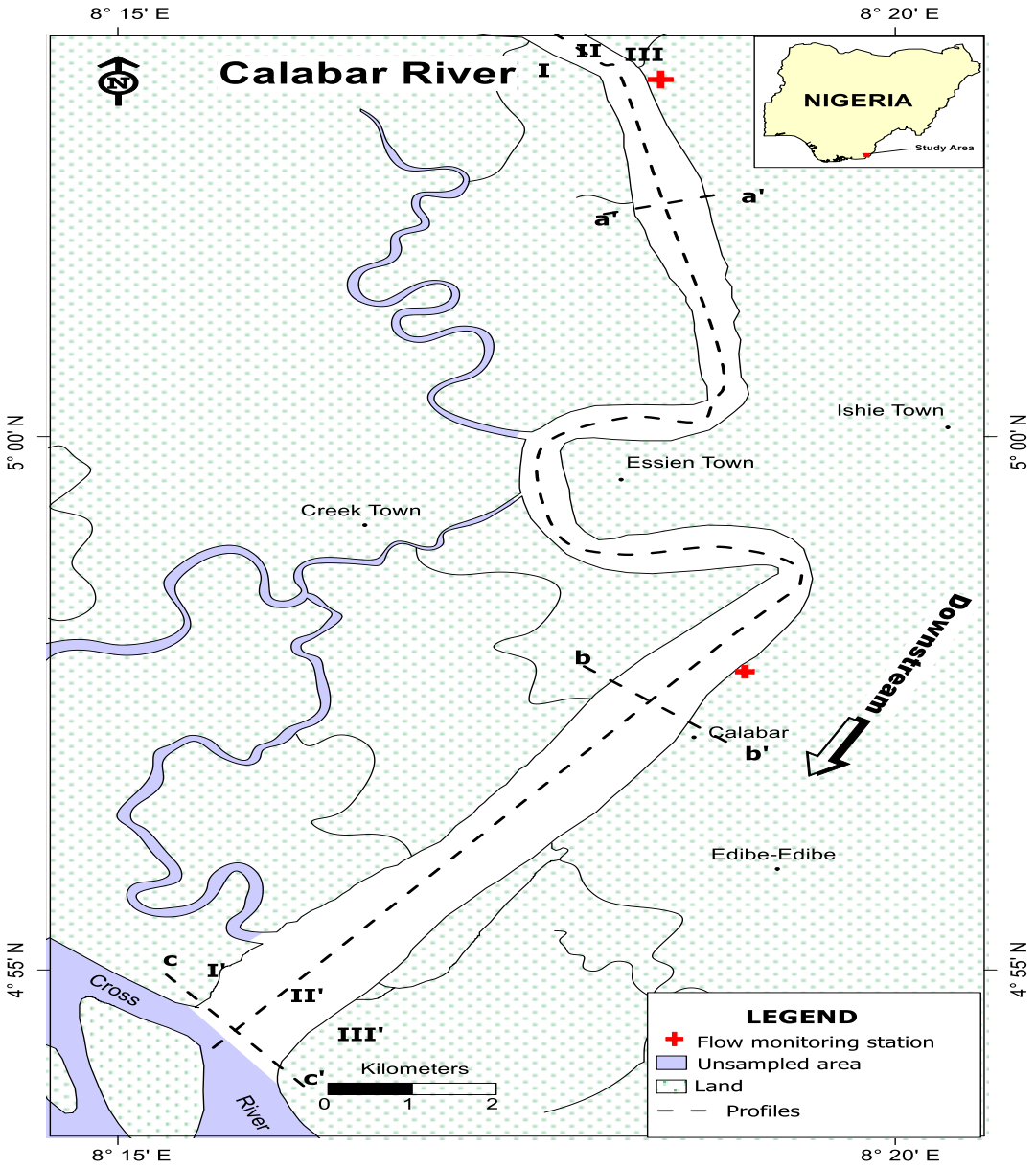

Fig. 22: Map of Calabar River showing cross-sectional transects

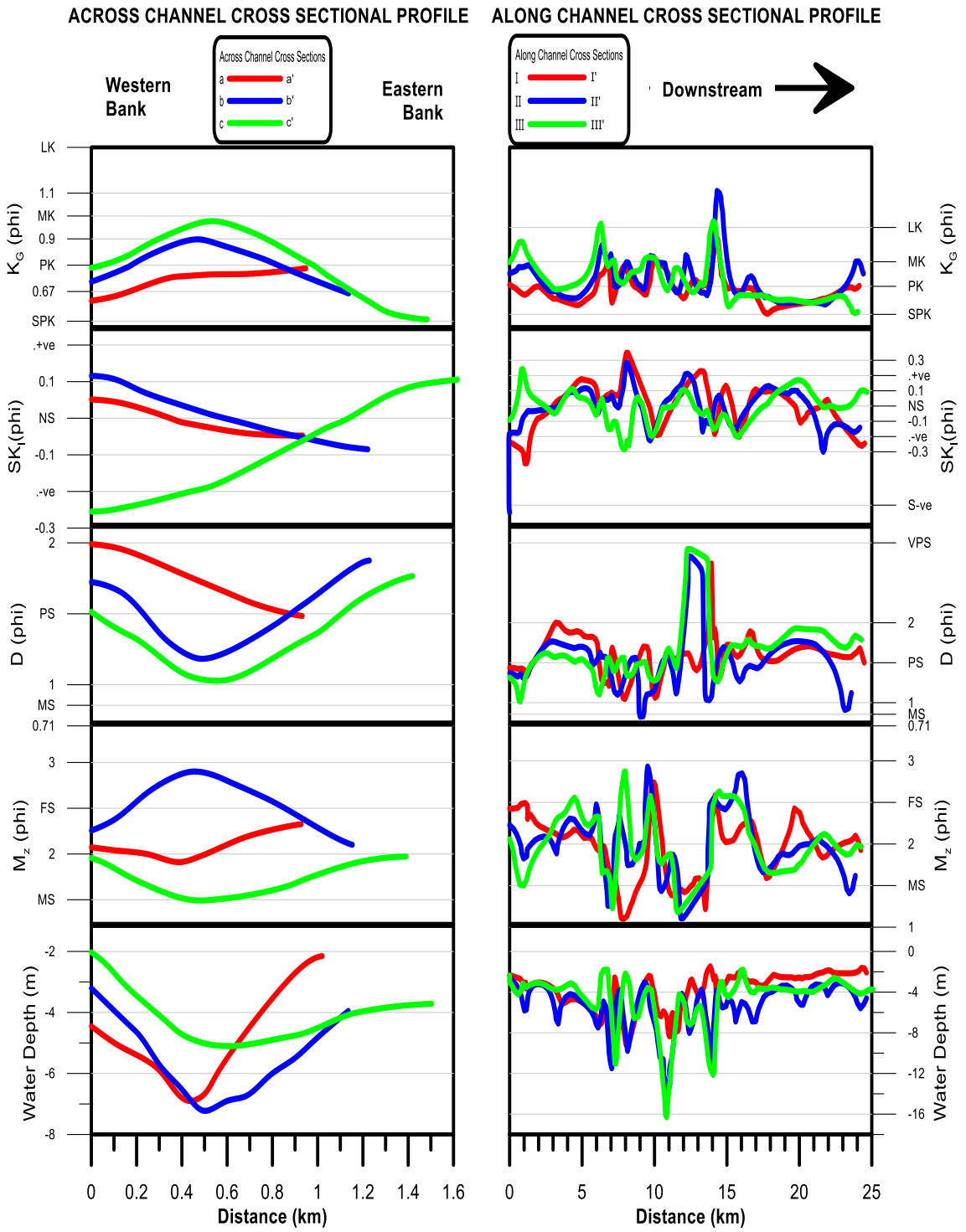

Fig. 23: Cross-sectional profiles of grain size statistical parameters in Calabar River

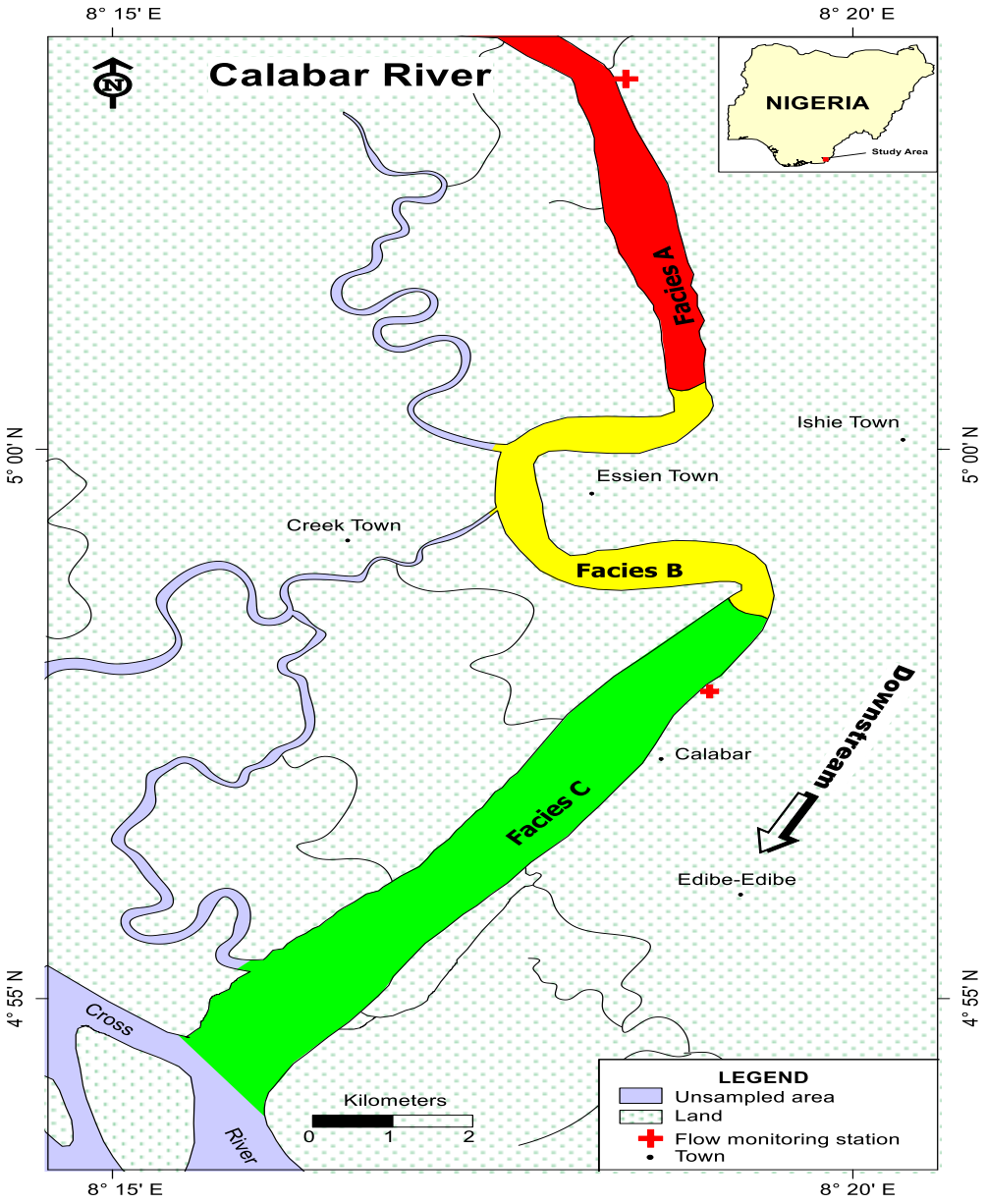

Fig. 24:Lithofacies map of Calabar River (Based on mean grain size)

Bivariate Relationships

Bivariate plots (Figs. 25–27) illustrate relationships among grain size parameters:

Mean Grain Size vs. Sorting: Sorting improves as mean size decreases in Facies A, improves with coarsening in Facies B, and deteriorates with fining in Facies C.

Mean Grain Size vs. Skewness and Kurtosis: Skewness shifts from near symmetric to negative with fining, while kurtosis varies from platykurtic to mesokurtic in Facies A and B, and strongly platykurtic in Facies C.

Sorting vs. Skewness and Kurtosis: Sorting deteriorates as sediments shift from symmetric to skewed, with kurtosis trending toward strongly platykurtic.

Skewness vs. Kurtosis and Depth: Sediments become more positive skewed as depth decreases in Facies A, while Facies B and C show increasing skewness with depth.

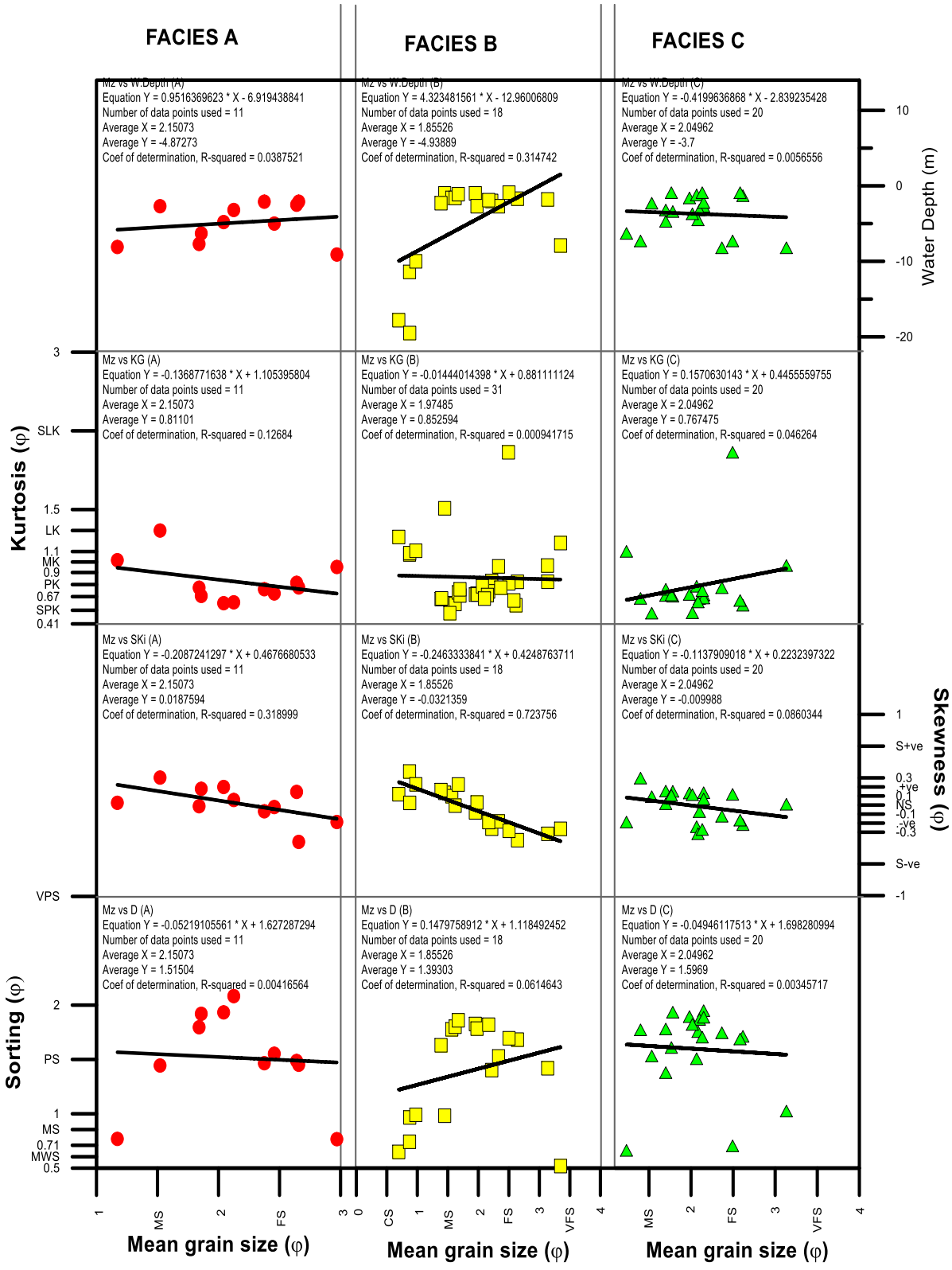

Fig. 25: Bivariate plots of mean grain size versus sorting, skewness, kurtosis and depth for Calabar River

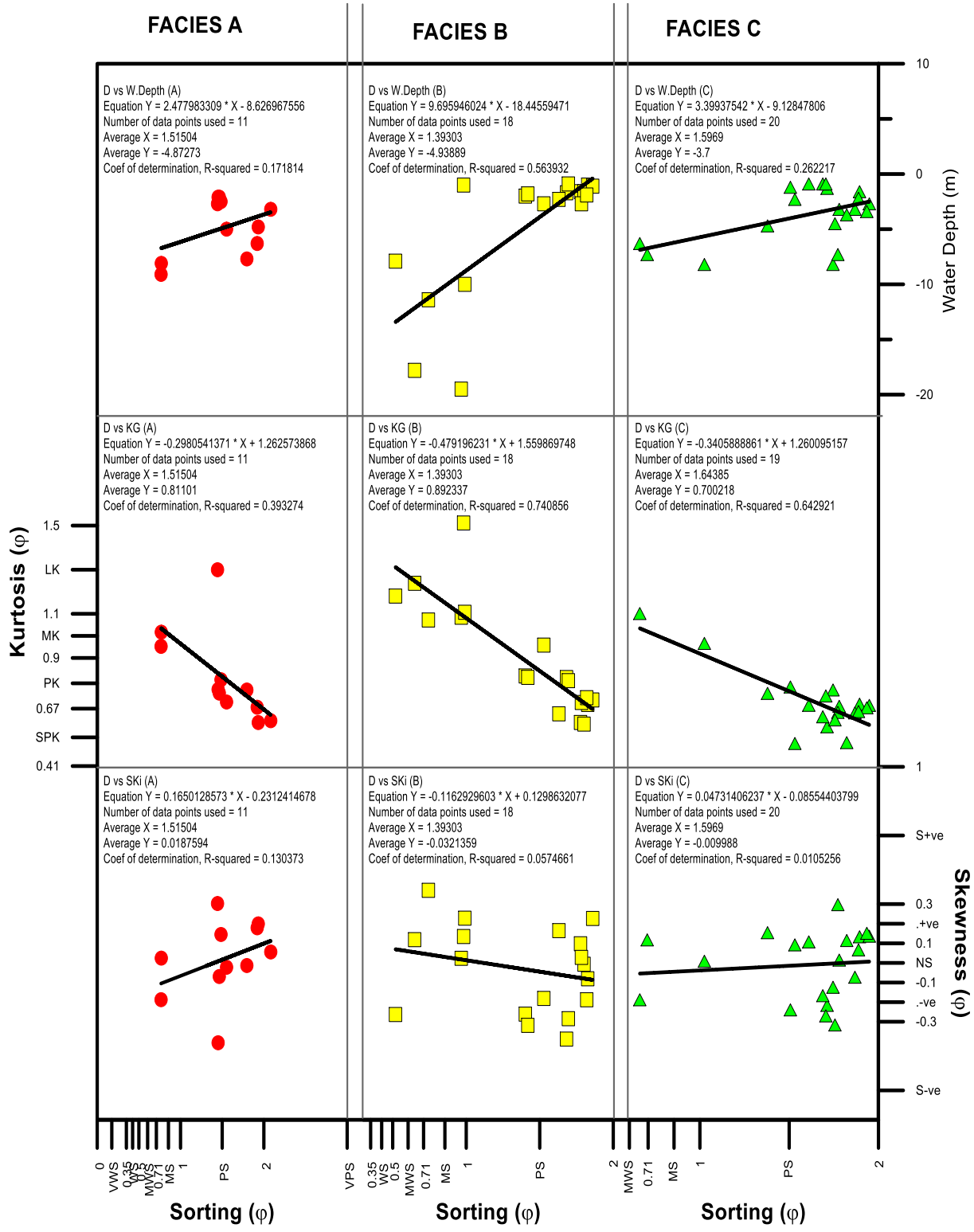

Fig. 26: Bivariate plots of sorting versus skewness, kurtosis and depth for Calabar River

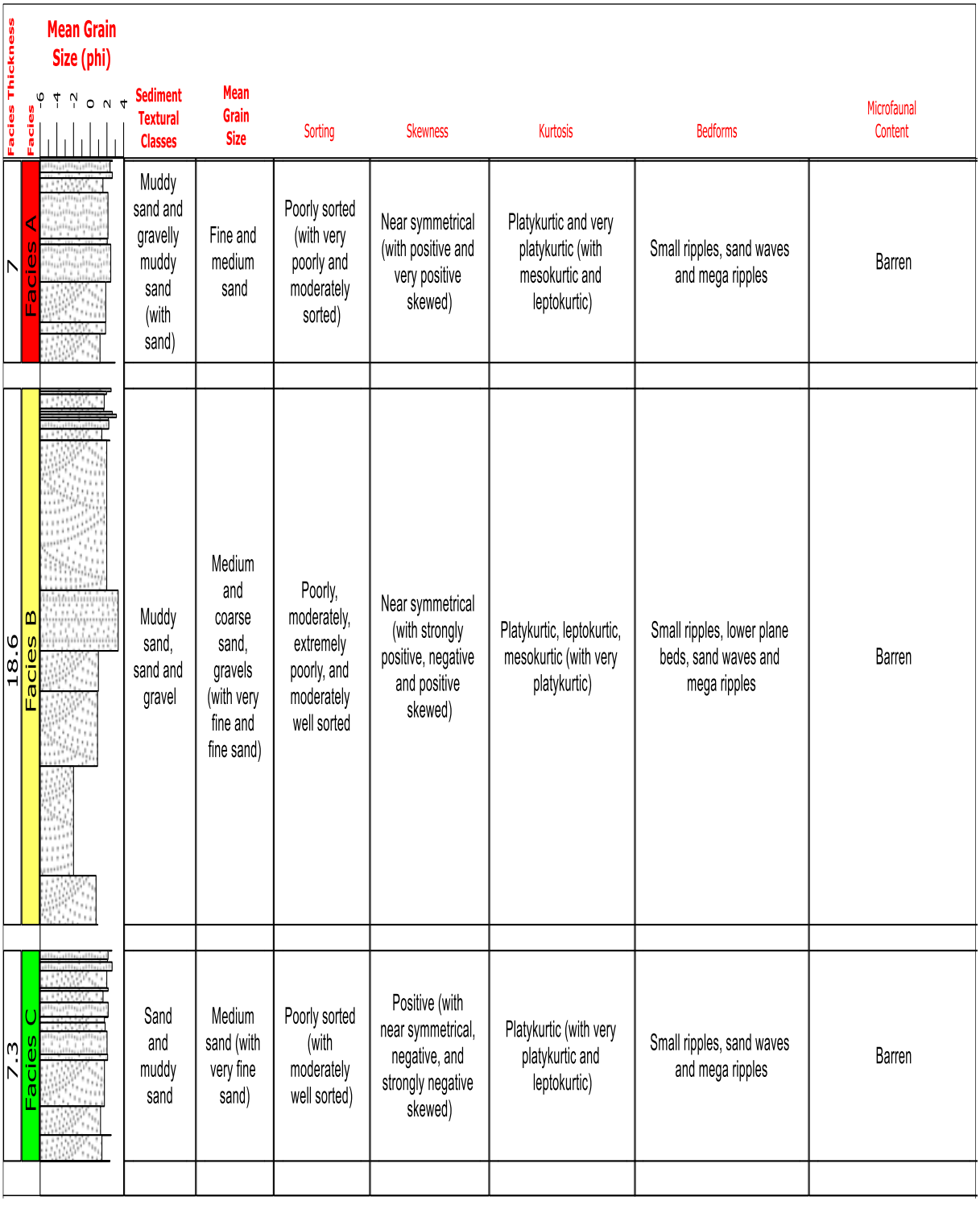

Fig. 28: A summary chart of the sedimentary facies of Calabar River

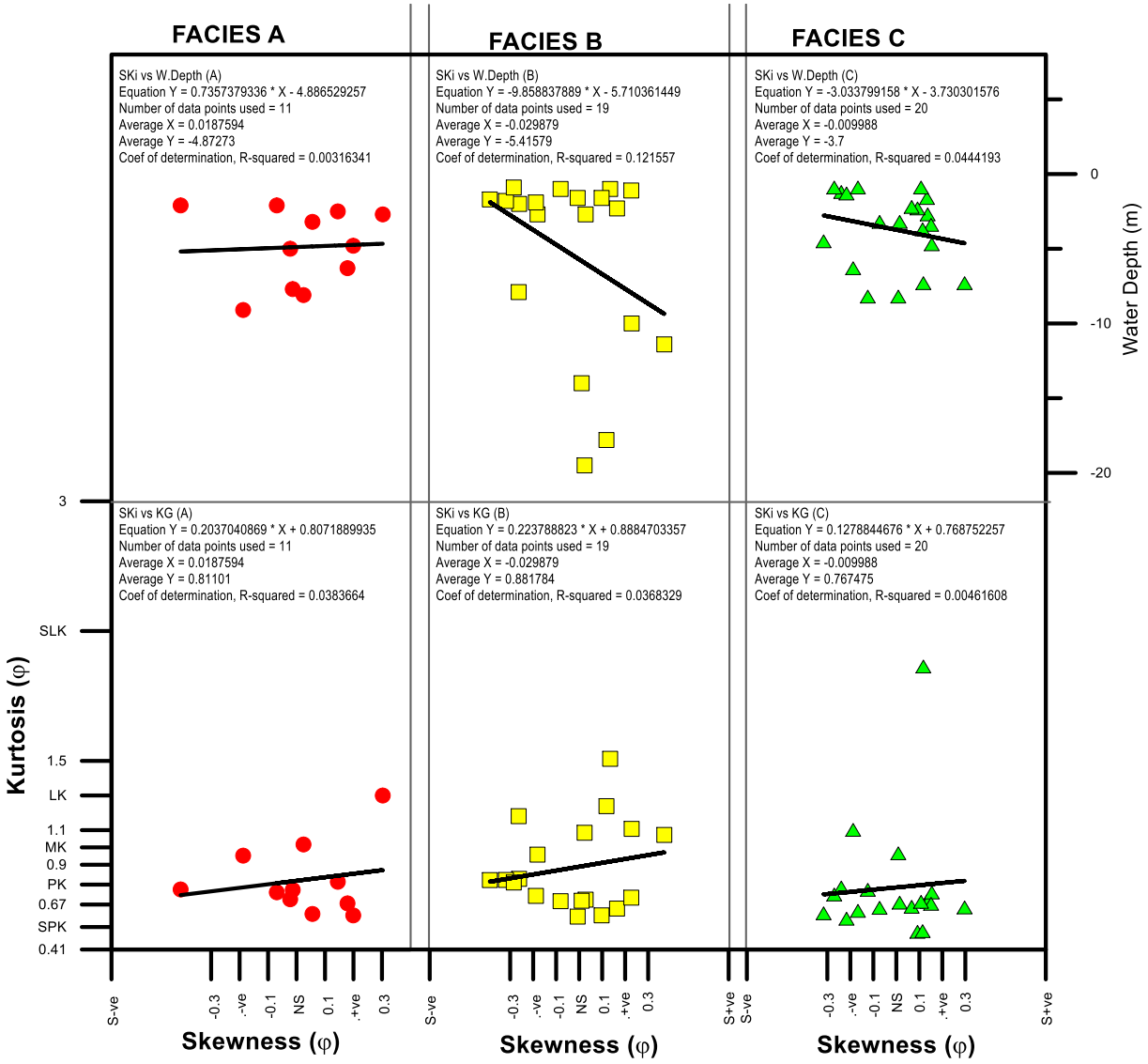

Fig, 27:Bivariate plots of skewness versus kurtosis and depth for Calabar River

3.2 Discussion

3.2.1 Relationship Between Grain Size Parameters and Hydrodynamics in the Calabar River

The distribution of grain size parameters within the Calabar River reflects strong influence of tidal asymmetry. Velocity profiles reveal an ebb-dominant regime, consistent with time–velocity asymmetry,and amplified by fluvial inputs from tributaries and rainfall. The observed ebb dominance is significant because it influences net sediment transport, grain size trends and facies architecture. The heterogeneous grain size distribution, ranging from mud to gravel, aligns with dynamic hydrodynamic processes. The predominance of sand and muddy sand reflects variations in tidal energy, while the coarsening trend toward the mid-channel suggests selective winnowing of finer fractions. This agrees with Semenuik (1981), who noted that tidal winnowing removes fine sediments to the banks, leaving coarser material in the main channel.

The upstream fining trend is interpreted as deposition by flood currents, whereas downstream coarsening reflects ebb-dominated

transport, consistent with Duncan & Dalrymple (2005) and Davis (1992). Sorting patterns highlight hydrodynamic control: improvement upstream and deterioration mid-channel suggest that changes in mean grain size directly affect sorting, in line with Chakrabarti (1971). Skewness patterns, with decreasing positive skewness downstream, indicate dependence on both grain size and energy conditions. Kurtosis trends toward leptokurtic values in the mid-channel as sorting deteriorates, contrasting with Folk & Ward (1957).

Recent studies confirm that tidal asymmetry strongly modulates sediment transport, with ebb dominance often producing net seaward sediment fluxes (Xie et al., 2024; Wenjing et al., 2025). In structurally modified or dredged tidal channels, asymmetry can be amplified, altering sediment pathways and facies distributions (Zhang et al., 2025). These findings suggest that the Calabar River's ebb dominance is not only natural but also enhanced by anthropogenic modifications such as dredging and sand mining.

3.2.2 Sedimentary Facies of the Calabar River

Three facies (A, B, and C; Figure 28) were delineated based on grain size parameters and textural attributes, reflecting spatial variations in hydrodynamic conditions and depositional processes. Facies A (Upstream): Extending laterally for ~6 km with a maximum depth of 10 m, this facies consists of fine-grained sands, muddy sands, and gravelly muddy sands. The sediments are poorly sorted, near-symmetric, and predominantly platykurtic, deposited under relatively lower-energy, flood-dominated conditions.

Facies B (Central): With a lateral extent of ~8 km and a maximum depth of 20 m, this facies comprises medium sands with patches of coarse and gravelly sediments. Sorting is poor, and skewness varies between positive and negative, reflecting alternating flood and ebb influences consistent with tidal asymmetry. Platykurtic sands dominate, with localized mesokurtic patches. This facies represents the highest-energy zone of the channel.

Facies C (Downstream): Extending ~10 km with a maximum depth of 8 m, this facies is dominated by medium sands and muddy sands, with small patches of fine sands. Sediments are poorly sorted, near-symmetric, and strongly platykurtic, deposited under ebb-dominant conditions.

This tripartite facies distribution aligns with established tidal channel frameworks, where upstream facies reflect flood deposition, central facies mark peak tidal energy zones, and downstream facies record ebb-dominated transport. The succession is comparable to models proposed by Nichols, Johnson, & Peebles (1991) and Cant & Walker (1978). Recent work emphasizes how tidal multi-asymmetry produces heterogeneous facies mosaics in estuarine systems (Zhang, Li, & Huang, 2025).

Anthropogenic activities further influence facies development. Dredging has deepened central portions of the channel, enhancing energy gradients and promoting coarser facies. Sand mining disrupts sediment supply, accelerating facies transitions downstream. These processes highlight the need to integrate human impacts into facies models, as modern tidal rivers increasingly reflect both natural and anthropogenic dynamics.

3.2.3 Broader Implications for Paleoenvironmental Reconstruction

The integration of grain size statistics with facies models provides an effective approach for reconstructing ancient tidal systems. The Calabar River demonstrates how tidal asymmetry, hydrodynamic gradients, and anthropogenic modification interact to shape facies architecture. Recognizing these signatures in the rock record can improve interpretations of ancient tidal rivers and estuarine deposits, particularly in meso-tidal settings.

The facies heterogeneity observed in the Calabar River underscores the importance of high-resolution sampling and statistical analysis. Bimodal grain size distributions, skewness variability, and kurtosis trends provide diagnostic markers of tidal asymmetry that can be applied to paleoenvironmental reconstructions. As recent studies emphasize, tidal asymmetry is a critical driver of residual sediment transport and facies heterogeneity (Wenjing et al., 2025; Xie et al., 2024). The Calabar River exemplifies how tidal asymmetry, facies variability, and anthropogenic modification converge to produce complex sedimentary architectures. These insights strengthen the application of facies models to both modern and ancient tidal systems, advancing sedimentological and paleoenvironmental research.

5.0 Conclusion

This study has demonstrated the close relationship between hydrodynamic conditions and grain size statistical parameters in the Calabar River. The ebb-dominant tidal regime, reinforced by fluvial inputs, exerts a strong control on sediment transport and facies development. Grain size distributions, sorting, skewness, and kurtosis collectively reflect the influence of tidal asymmetry, with flood currents contributing to upstream fining and ebb currents driving downstream coarsening.

Three distinct sedimentary facies: A, B, and C were delineated, representing the upstream, central, and downstream portions of the channel. Facies A records flood-dominated deposition of fine sands and muddy sands; Facies B reflects peak tidal energy with medium sands and gravelly patches; and Facies C captures ebb-dominated deposition of medium sands and muddy sands. Together, these facies illustrate how tidal asymmetry and hydrodynamic gradients shape facies architecture in meso-tidal systems.

Beyond its local significance, the Calabar River provides a valuable modern analogue for interpreting ancient estuarine deposits. The integration of grain size statistics with facies models enhances paleoenvironmental reconstruction, offering insights into depositional processes in tidal rivers subject to both natural dynamics and anthropogenic modification.

6.0 References

Antia, V. I., Emeka, N. C., Ntekim, E. E. U. & Amah, E. A. (2012). Grain size distribution and flow measurements in Qua-Iboe River estuary and Calabar River, South-East Nigeria. *European Journal of Scientific Research,* 67 , 2, pp. 223-239.

Awasthi, A. K. (1970). Skewness as an environmental indicator in the Solani River System of Roorke, India. *Journal of Sedimentary Geology,* 4, pp. 177-183.

Agbiji, N. M., Agunwamba, J. C., & Eshiet, K. I. I. (2024). Trend analysis of climatic variables in the Cross River Basin, Nigeria. *Geosciences, 14,* 6, pp. 172. https://doi.org/10.3390/geosciences14060172

Biggs, R. B. & Howell, B. A. (1984). The estuary as a sediment trap: Alternate approaches to estimating its filtering efficiency. In N. C. Emeka, V. I., Antia, A. J., Ukpong, E. A., Amah and E. E. U. Ntekim, A study on the sedimentology of tidal rivers: Calabar and Great Kwa, South-East Nigeria. *European Journal of Scientific Research*, 47, 3, pp. 370-386.

Bricker, O. P. & Troup, B. N. (1975). Sediment water exchange in Chesapeake Bay. *Estuarine Research*, 1, pp. 3-11.

Cant, D. J. & Walker, R. G. (1978). Fluvial processes and facies sequences in the studied braided South Saskatchewan River. *Sedimentology*, 26, pp. 508-651.

Chakrabarti, A. (1971). Studies on sediment movement at the entrance of a tidal river. *Journal of Sedimentary Geology,* 6, pp. 111-127.

Cross River Climate Data. (2025). *Cross River, NG climate zone, monthly weather averages and historical data*. Retrieved May 26, 2026, from https://www.weather-atlas.com/en/nigeria/cross-river

Dalrymple, R. W., & Choi, K. (2007). Morphologic and facies trends through the fluvial–marine transition in tide-dominated depositional systems: A schematic framework for environmental and sequence-stratigraphic interpretation. *Sedimentary Geology, 202, 3,* pp. 469–491. https://doi.org/10.1016/j.sedgeo.2007.09.001

Davis, R. A. (1992). *Depositional systems: An introduction to sedimentology and stratigraphy*. New Jersey: Prentice-Hall, 306p.

Debekeme, P., Antia, E., Soronnadi-Ononiwo, G. C., & Oghale, L. O. (2022). Grain size distribution of a modern tidal river: A case study of Calabar River, South-South Nigeria. *International Journal of Science and Research, 1,* 4, pp. 123–134.

DeRaaf, J. F. M. & Boersma, J. R. (1971). Tidal deposits and their sedimentary structures. *Geologie en Mijnbouw,* 15, pp. 479-504.

Duncan, M. & Dalrymple, R. (2005). A sedimentological comparison of tide-dominated estuarine and tide-dominated deltaic deposit: a sub-surface perspective. Retrieved June 16, 2005 from www.searchanddiscovery.com/abstracts/html/2005.iju

Emeka, N. C., Antia, V. I., Ukpong, A. J., Amah, A. E. & Ntekim, E. E. U. (2010). A study on the sedimentology of tidal rivers: Calabar and Great Kwa, South-East Nigeria. *European Journal of Scientific Research*, 47, 3, pp. 370-386.

Folk, R. L. & Ward, W. C. (1957). Brazos River bar: A study in the significance of grain size parameters. *Journal of Sedimentary Petrology,* 27, pp. 3-27.

Folk, R. L. (1980). The distinction between grain size and mineral composition in sedimentary rocks. *Journal of Geology*, 62, pp. 344-359.

Friedman, G. M. (1961). Distinction between dune, beach and river sands from their textural characteristics. *Journal of Sedimentary Petrology*, 31, pp. 514-529.

Friedman, G. M. & Sanders, J. E. (1978). *Principles of sedimentology.* New York: John Wiley and Sons, 500p.

Green, M. O. (2011). Sediment transport in estuaries: A review. *Estuarine, Coastal and Shelf Science, 92*, 3, pp. 409–421. https://doi.org/10.1016/j.ecss.2010.12.033

Gujar, A. R., Angusamy, N. & Rajamanickam, G. V. (2007). Characterization of opaques off Konkan Coast Maharashtra, central west coast of India. *Journal of Minerals, Materials Characterization and Engineering*, 6, 11, pp. 53-67.

Hall, M. J., Nadeau, J. E. & Nicilich, M. (1987). The use of trace metal content to verify sediment transport from Delaware Bay on to the New Jersey inner shelf. *Journal of Coastal Research,* 3, pp. 469-474.

Hayes M. O. (1975). Morphology of sand accumulation in estuaries: An introduction to the symposium. In H. G. Reading, *Sedimentary environments and facies*. London: Blackwell Scientific Publications, 557p.

Hijmans, R. J. (2011). Spatial data. Retrieved December 12, 2011 from www.diva-gis.org/Data.

Kamaruzzaman, B. Y., Shazili, N. A. & Mohd Lokman, H. (2002). Particle size distribution in the bottom sediments of the Kemaman River estuarine system, Malaysia. *Pertanika Journal of Tropical Agricultural Science,* 25, 2, pp. 149 –155.

Longhitano, S., Rossi, V. M., & Chiarella, D. (2025). Modern and ancient tidal sedimentary systems in the era of energy transition: Introduction to the special volume of *The Depositional Record*. *The Depositional Record, 11, 5, pp.* 1542–1553. https://doi.org/10.1002/dep2.70001

Malvarez, G., Cooper, J. A. & Jackson, D. W. (2001). Relationship between waves and tidal flat sedimentation. *Journal of Sedimentary Research*, 71, 5, pp. 705-712.

Martins, L. R. (2003). Recent sediments and grain-size analysis. *Sedimentological Research Group,* 1, pp. 90-105.

Mead, S. & Moores, A. (2005). Estuary sedimentation: A review of estuarine sedimentation in the Waikato region. Retrieved June 21, 2005 from www.waikatoregion.govt.nz

Nichols, M. M., & Biggs, R. B. (1985). Estuaries. In R. A. Davis Jr. (Ed.), *Coastal Sedimentary Environments* (pp. 77–186). Springer. https://doi.org/10.1007/978-1-4612-5078-43

Nichols, M., Johnson, G. & Peebles, P. (1991). Modern sediments and facies model for a micro-tidal coastal plain estuary: The James Estuary, Virginia. *Journal of Sedimentary Research*, 61**,** pp. 883-889.

Nigerian Geological Survey Agency (2007). Geological map of Nigeria. Federal Government of Nigeria.

Okon, L.-U. E., Ekpang, P. U., Nganje, T. T., Akpan, E. B., & Iwuagwu, E. P. (2025). Deciphering litho-facies heterogeneity and sedimentological variability in tropical tidal flats of the Calabar and Great Kwa Rivers, Nigeria: Implications for coastal sediment dynamics. *Asian Journal of Geographical Research, 8, 3, pp* 266–284. https://doi.org/10.9734/ajgr/2025/v8i3291

Semenuik, V. (1981). Sedimentology and stratigraphic sequence of a tropical tidal flat, King Sound, Northwestern Australia. *Sedimentary Geology, 29,* pp. 195-221.

Valia, H. S. & Cameron, B. (1977). Skewness as paleoenvironmental indicator. *Journal of Sedimentary Petrology,* 47, 2, pp. 784-793.

Van den Berg, J. H., Boersma, J. R. & Van Gelder, A., (2007). Diagnostic sedimentary structures of the fluvial-tidal transition zone-evidence from deposits of the Rhine and Meuse. *Netherlands Journal of Geosciences*, 86,3, pp. 287-306.

Tessier, B., Billeaud, I., & Lesueur, P. (2010). Facies architecture of tidal channel fills: Insights from modern and ancient estuarine systems. *Sedimentology, 57,* 6, pp. 1550–1572. https://doi.org/10.1111/j.1365-3091.2010.01156.x

Wenjing, Z., Liu, H., & Chen, Y. (2025). Floc size asymmetry modulated by tidal dynamics drives net landward sediment transport in a man-made tidal channel. *Marine Geology, 488*, 107615. https://doi.org/10.1016/j.margeo.2025.107616

Xie, J., Feng, X., & Gao, G. (2024). Variation of suspended sediment caused by tidal asymmetry and wave effects. *Ocean Modelling, 192*, 102454. https://doi.org/10.1016/j.ocemod.2024.102454

Zhang, Y., Li, P., & Huang, J. (2025). Multi-asymmetry on residual sediment transport in the branching channels of the Yangtze Estuary. *Journal of Hydrology, 655*, 132947. https://doi.org/10.1016/j.jhydrol.2025.132947

Declarations:

Conflict of interest

The authors declare that they have no conflict of interest

Data availability

All data used in this study will be readily available to the public.

Consent for publication

Not Applicable.

Ethical consideration

Not applicable

Competing interests

The authors declared no conflict of interest.

Authors' Contributions

The authors contributed collectively to the conception and design of the study, field sampling, tidal-current measurements, bathymetric surveys, laboratory grain-size analyses, data interpretation, facies

characterization, and paleoenvironmental reconstruction. Chimezie Emeka led the research and manuscript preparation. Victoria Emeka, Edak Agi-Odey, Aniekan Ukpe, and Celsus Agim contributed to data acquisition, analysis, literature review, manuscript revision, and approval of the final version.